GModel
SBMB-3729; No. of Pages 6
ARTICLE IN PRESS

Journal of Steroid Biochemistry & Molecular Biology xxx (2011) xxx–xxx

Contents lists available at SciVerse ScienceDirect

Journal of Steroid Biochemistry and Molecular Biology

journal homepage: www.elsevier.com/locate/jsbmb

LIN28: A regulator of tumor-suppressing activity of *let-7* microRNA in human breast cancer

Minako Sakurai[a], Yasuhiro Miki[a], Mariko Masuda[a], Shuko Hata[a], Yukiko Shibahara[a], Hisashi Hirakawa[b], Takashi Suzuki[a], Hironobu Sasano[a,*]

[a] *Department of Pathology, Tohoku University, Graduate School of Medicine, 2-1 Seiryo-machi, Aoba-ku, Sendai, Miyagi 980-8575, Japan*
[b] *Department of Surgery, Tohoku Kousai Hospital, Japan*

ARTICLE INFO

Article history:
Received 29 June 2011
Received in revised form 20 October 2011
Accepted 21 October 2011

Keywords:
Breast cancer
LIN28
LIN28B
let-7

ABSTRACT

A tumor-suppressor gene, *let-7* microRNA (miRNA) family, is often inactivated in various human malignancies. LIN28 is a RNA-binding protein that has been well characterized for regulation of *let-7* maturation in undifferentiated embryonic stem cells at post-transcriptional level. Oncogenic regulation of *let-7* miRNAs has been demonstrated in several human malignancies but their correlation with LIN28 has not been studied in breast cancer. We therefore explored a possible mechanism of tumorigenesis in breast carcinoma tissue via an alternation of *let-7* miRNA precursor processing by LIN28 in this study. A total of 26 breast cancer surgical pathology specimens were evaluated for LIN28 and LIN28B expression using immunohistochemistry. We then isolated carcinoma cells in 21 cases using laser capture microdissection, and the miRNAs from these samples were profiled using PCR array analysis. LIN28 status was positively correlated with ERα, PR, and Ki-67 status and inversely correlated with HER2 status. These results suggest the possible involvement of LIN28 in regulation of sex steroid dependent cell proliferation of breast carcinoma cells. We further demonstrated that expression of *let-7a*, *let-7c*, *let-7d* ($P=0.026$) and *let-7f* ($P=0.016$) were inversely correlated with those of LIN28. These results also suggest that LIN28 promotes tumorigenic activity by suppressing *let-7* miRNA maturation in breast carcinoma cells.

This article is part of a Special Issue entitled 'Steroids and cancer'.

1. Introduction

MicroRNAs (miRNAs) are a class of small non-coding RNAs, 22 nucleotides long on the average, and bind to their complementary sequences on target downstream messenger RNAs (mRNAs) serving as post-transcriptional regulators [1]. Recent reports clearly indicate that miRNAs are involved in multiple regulatory roles and frequently repressed in various human malignancies [2,3]. The lethal-7 (*let-7*) gene is one of the highly conserved miRNAs, which consists of ten mature *let-7* family sequences in humans [1]. The *let-7* miRNAs have been demonstrated to regulate multiple oncogenes such as HMGA2, c-Myc, RAS, and cyclinD1 [3–6]. This regulation is demonstrated by recent results of *in vitro* experiments in lung cancer demonstrated that *let-7* negatively regulated RAS, and subsequently resulted in suppression of lung carcinoma cell growth [5,7].

LIN28 is a RNA-binding protein which inhibits premature *let-7* precursor processing. LIN28 and its homolog, LIN28B have been known to regulate all *let-7* family members through maturation process and cellular differentiation [8]. As an example, LIN28 was reported to act as trans-acting regulators which bind *let-7* pre-miRNA to block its maturation in embryonic stem cells [9]. This particular function of *let-7* was used in the process of establishing induced pluripotent stem (iPS) cells from human fibroblasts in order to enhance the efficiency of cellular formation by the group of Thompson [10]. In particular, Balzer et al. [11] identified significant interactions between LIN28 and three *pre-let-7* miRNAs; *let-7 a*, *g*, and *f* by *in vitro* experiment. A number of studies have also portrayed an association between LIN28 and *let-7*, with particular emphasis upon their involvement in cellular processes such as differentiation and proliferation [12,13]. In particular, the status of LIN28/LIN28B expression was reported to play important roles in biological/clinical behavior of human lung and ovarian malignancies in recent studies [14,15].

The majority of breast cancer is estrogen-dependant. Reduced expression of *let-7* family was reported in human breast cancer tissues [16]. However, a correlation between *let-7* and LIN28 in breast carcinoma cells or tissues has not been confirmed. Therefore, we examined the expression of LIN28 and LIN28B in breast

Abbreviations: miRNA, microRNA; ER, estrogen receptor; PR, progestine receptor; HER2, human epidermal growth factor 2; LCM, laser capture microdissection.

* Corresponding author. Tel.: +81 022 717 8050; fax: +81 022 717 8051.
E-mail address: hsasano@patholo2.med.tohoku.ac.jp (H. Sasano).

0960-0760/$ – see front matter © 2011 Elsevier Ltd. All rights reserved.
doi:10.1016/j.jsbmb.2011.10.007

cancer patients and evaluated their correlation with the post-transcriptional regulation by *let-7* using miRNA PCR array in order to understand their clinicopathological significance in breast cancer patients.

2. Materials and methods

2.1. Patients and tissues

A total of 26 primary breast cancer specimens obtained from Japanese female patients who underwent surgical treatment from 2004 to 2010 in Tohoku Kosai Hospital (Sendai, Japan) were available for examination in this study. The age of the subjects ranged from 31 to 86 years (median: 57 years), and 21 cases (41–86 years: median 58.6 years) were selected for PCR array analysis among these 26 cases. Tissues were fixed with 10% formalin for 24–48 h at room temperature and were embedded in paraffin. Research protocol for this study was approved by the ethics committee of both Tohoku University, Graduate School of Medicine (2010-572) and Tohoku Kosai Hospital (H17.8.5).

2.2. Immunohistochemistry of LIN28/LIN28B

Immunohistochemical staining was performed using a biotin-streptavidin method with Histofine kit (Nichirei Co. Ltd., Tokyo, Japan). The slides were deparaffinized in xylene, followed by hydration through a series of alcohol. Hydrogen peroxidase was used to block intrinsic peroxidase activity. Following the application of primary antibodies, the reacted sections were incubated at 4 °C for 24 h. The primary antibodies, LIN28 (55CT58.12.1: mouse monoclonal antibody), and LIN28B (rabbit polyclonal antibody) were commercially obtained from Abcam Ltd. (Cambridge, UK). Human testis tissue was used as a positive control of immunostaining [17].

The following primary antibodies were used for other immunohistochemical analysis: monoclonal antibodies for estrogen receptor α (ER; ER1D5; Immunotech, Marseille, France), progesterone receptor (PR; MAB429; Chemicon International Inc., CA, US), and Ki-67 (MIB-1; DakoCytomation Co. Ltd., Kyoto, Japan), and rabbit polyclonal antibody for HER2/*neu* (AO485; DakoCytomation).

2.3. Evaluation of LIN28/LIN28B immunoreactivity

The relative immunointensity of both LIN28 and LIN28B in the cytoplasm of carcinoma cells was independently evaluated by two of the authors (M.S. and Y.M.) as follows: negative (0) when their relative immunointensity was lower than the positive control, and positive (1) when their relative immunointensity was equal or more intense than the positive control of immunostain. The immunostained slides were separated into four different areas; top right, top left, bottom right, and bottom left. For evaluation, we have modified a method introduced in a report by Hata et al. [18]. The average immunointensity obtained in these four different areas of the specimens was determined as the relative immunointensity of the cases.

Immunoreactivity of ERα, ERβ, PR, and Ki-67 was detected in the nuclei, and counted in more than 1000 breast carcinoma cells. Labeling index (LI in %) was used to estimate a proportion or ratio of immunoreactivity. The cases with less than 10% were considered as ERα-, ERβ-, PR-, and Ki-67 negative as previously reported [19]. An evaluation of HER2 was employed in accordance with Hercep Test (DAKO) grading system. HER2 immunoreactivity was classified as positive when membrane was stained either moderately or strongly (equivalent to score 2 and 3 respectively, based on Hercep Test, DAKO) in more than 10% of carcinoma cells.

2.4. miRNA PCR array

Human Cancer RT^2 Profiler PCR Array system (QIAGEN, Mannheim, Germany) was used as demonstrated in previous reports in order to measure expression of *let-7* family in a quantitative fashion in isolated breast carcinoma cells [20]. Laser capture microdissection was carried out to isolate carcinoma cells from 8 μm formalin fixed and paraffin embedded tissue sections (FFPE) using MMI CellCut (Molecular Machines and Industries, Flughofstrasse, Glattbrug, Switzerland). Approximately 5000 carcinoma cells were obtained from individual tissue sections. These isolated carcinoma cells were deparaffinized at 60 °C for 3 h. Extraction of miRNA was performed as instructed by Pure Link miRNA Isolation Kit (Invitrogen, Carlsbad, CA), followed by cDNA synthesis using RT^2 miRNA First Strand Kit (QIAGEN). qRT-PCR was employed with ABI7500 real-time PCR system (Applied Biosystems, Forster city, CA, USA) to determine expression levels of *let-7* miRNAs using RT^2 profiler PCR Array Data Analysis for statistical analysis (http://pcrdataanalysis.sabiosciences.com/pcr/arrayanalysis.php).

2.5. Statistical analysis

Stat View 5.0J Software (SAS Institute Inc., NC, USA) was used for analytical findings of clinicopathological features in the cases examined. The values for patient's age, ERα LI, ERβ LI, and PR LI were represented as the mean ± SD. For hierarchical clustering analysis, LIN28 expression of each sample was categorized based upon its immunoreactivity, compared with results of microarray analysis of *let-7* family. The tree structures were formulated using TreeView programs (Stanford University, Palo Alto, CA; Ref. [24]) according to the degree of similarity. We compared the results of PCR array with those of immunohistochemistry using Bonferroni/Dunn and Mann–Whitney *U* test. The significance of each value was determined when *P* value was less than 0.05. The statistical differences between LNI28/LIN28B and clinicopathological parameters were determined using Chi-square analysis; 95% confidence interval calculated for confirmation of statistical significance.

3. Results

3.1. Localization of LIN28 and LIN28B in breast carcinoma tissues

We first evaluated an association between LIN28/LIN28B and clinicopathological features of individual cases. LIN28 and LIN28B immunoreactivity was detected in human testicular spermatocyte (data not present) as previously reported [17]. LIN28 and LIN28B immunoreactivity was predominantly detected in cytoplasm of breast carcinoma cells as illustrated in Fig. 1. Among 26 cases examined, the presence of LIN28 and LIN28B was detected in carcinoma cells of 16 cases and in epithelial cells of adjacent non-neoplastic mammary glands of all the cases examined, although the relative immunointensity of these non-neoplastic cells above was markedly weak compared to that of carcinoma cells.

3.2. LIN28 and LIN28B in breast cancer tissues

An association between LIN28 and clinicopathological parameters was summarized in Table 1. There was a significantly positive correlation between the LIN28 and ERα expression ($P = 0.007$ for LI, $P = 0.002$), PR ($P = 0.034$) and Ki-67 ($P = 0.049$), whereas the status of HER2 was inversely associated with LIN28 status ($P = 0.036$) of the cases examined. No significant correlation was detected between ERβ and LIN28. In addition, LIN28 and LIN28B ($P = 0.009$) were positively correlated in all the cases evaluated. An association between LIN28B and clinicopathological features was summarized in Table 2. There was a significantly positive association between

Please cite this article in press as: M. Sakurai, et al., LIN28: A regulator of tumor-suppressing activity of *let-7* microRNA in human breast cancer, J. Steroid Biochem. Mol. Biol. (2011), doi:10.1016/j.jsbmb.2011.10.007

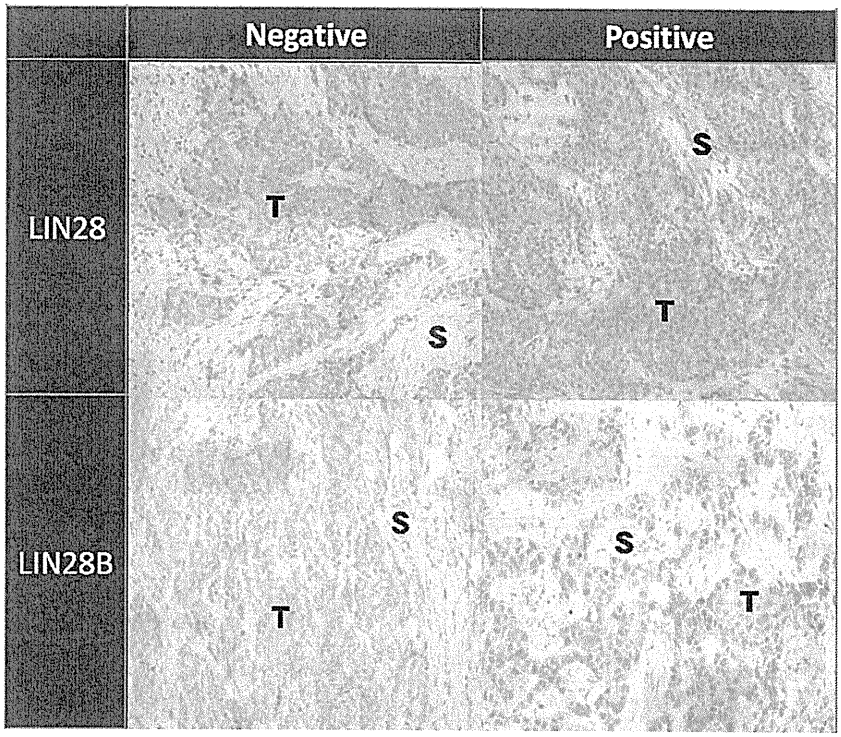

Fig. 1. Immnunolocalization of LIN28 and LIN28B in breast carcinoma tissues. A total of 26 specimens were classified according to the degree of relative immunointensity; negative (<control) and positive (≧ control) groups. Immunoreactivity of both LIN28 and LIN28B was detected predominantly in the cytoplasm of breast carcinoma cells. Testis was used as positive control. S, stromal cells; T, carcinoma cells, 100×.

Table 1
Clinicopathological characteristics of LIN28 in breast carcinoma cells.

Clinicopathological parameters	LIN28		*P*-value
	Negative ($n=10$)	Positive ($n=16$)	
Age LI (%)	54.40 ± 5.41	59.31 ± 2.57	0.367
ERα			
+	2 (7.69%)	13 (50.00%)	
–	8 (30.77%)	3 (11.54%)	**0.002**
ERα LI (%)	20.00 ± 12.27	61.19 ± 7.91	**0.006**
ERβ			
+	6 (23.08%)	6 (23.08%)	
–	4 (15.38%)	10 (38.46%)	0.262
ERβ LI (%)	22.30 ± 6.52	14.94 ± 4.14	0.325
PR			
+	2 (7.69%)	10 (38.46%)	
–	8 (30.77%)	6 (23.08%)	**0.034**
PR LI (%)	17.30 ± 11.16	25.75 ± 6.59	0.491
Ki67			
+	10 (38.46%)	11 (42.31%)	
–	0	5 (19.23%)	**0.049**
HER2			
+	5 (50.00%)	2 (12.50%)	
–	5 (50.00%)	14 (87.50%)	**0.036**
LIN28B			
+	3 (11.54%)	13 (50.00%)	
–	7 (26.92%)	13 (11.54%)	**0.009**

LI (%), labeling index in %; $P \leqq 0.05$ is indicated in bold.

LIN28B and Ki-67 status ($P = 0.049$), but no other significant associations were detected.

3.3. Expression of let-7 family and its correlation with LIN28 and LIN28B

Histopathological examination revealed an important interaction between the status of LIN28 and hormone receptors in breast carcinoma cells as described above. We therefore focused upon the effects of LIN28 towards *let-7* miRNA family in human breast carcinoma cells. Hierarchical clustering analysis of PCR array demonstrated that the status of *let-7* miRNA expression tended to be correlated with that of LIN28 immunoreactivity in human breast carcinoma cells (Fig. 2A). LIN28 positive group tended to be associated with reduced expression of *let-7*, whereas cases with negative LIN28 status tended to be associated with increased expression of the great majority of *let-7* miRNAs. Fig. 2B–I represented miRNA concentration according to LIN28 expression of the cases. Of

Table 2
Clinicopathological characteristics of LIN28B in breast carcinoma cells.

Clinicopathological parameters	LIN28B		*P*-value
	Negative ($n=10$)	Positive ($n=16$)	
Age LI (%)	56.5 ± 3.57	58.00 ± 3.66	0.785
ERα			
+	5 (19.23%)	10 (38.46%)	
–	5 (19.23%)	6 (23.08%)	0.530
ERα LI (%)	38.70 ± 12.68	49.50 ± 9.97	0.509
ERβ			
+	4 (15.38%)	8 (30.77%)	
–	6 (23.08%)	8 (30.77%)	0.619
ERβ LI (%)	16.20 ± 5.45	18.75 ± 4.81	0.735
PR			
+	5 (19.23%)	7 (26.92%)	
–	5 (19.23%)	9 (34.61%)	0.756
PR LI (%)	26.20 ± 10.61	20.19 ± 6.98	0.625
Ki67			
+	10 (38.46%)	11 (42.31%)	
–	0	5 (19.23%)	**0.049**
HER2			
+	4 (40.00%)	3 (18.75%)	
–	6 (60.00%)	13 (81.25%)	0.235

LI (%), labeling index in %; $P \leqq 0.05$ is indicated in bold.

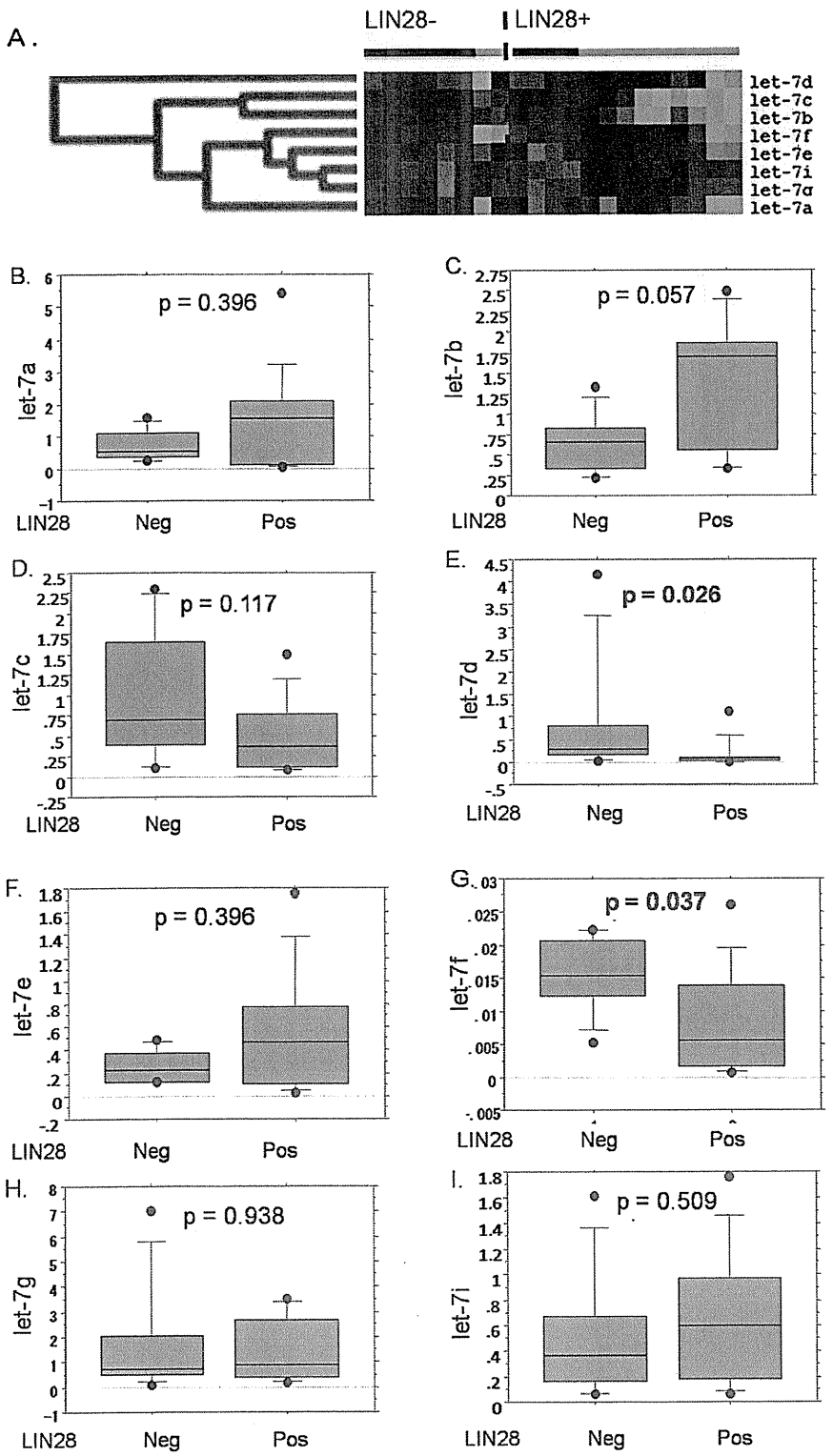

Fig. 2. Expression of *let-7* miRNA and LIN28. (A) Hierarchical cluster analysis demonstrating expression of *let-7* miRNA family in 21 breast carcinoma cases. The cases were classified into two groups; LIN28 (−) and LIN28 (+). The black bars represent high expression of *let-7* miRNAs, and the grey bars represent low expression of *let-7* miRNAs. Red, high miRNA expression; green, low miRNA expression. (B)–(I) The box plot representing relative mature miRNA expression in *y*-axis, and LIN28 expression in *x*-axis. A horizontal line in the box plot illustrates the median value. The upper and lower bars indicate the 90th and 10th percentiles, respectively. The statistical analysis was performed using a Mann–Whitney *U* test. $P \leqq 0.05$ is indicated in bold. (For interpretation of the references to color in this figure legend, the reader is referred to the web version of this article.)

Please cite this article in press as: M. Sakurai, et al., LIN28: A regulator of tumor-suppressing activity of *let-7* microRNA in human breast cancer, J. Steroid Biochem. Mol. Biol. (2011), doi:10.1016/j.jsbmb.2011.10.007

eight *let-7* miRNA family members, the level of *let-7d* ($P = 0.026$, 0.184-fold) and *let-7f* ($P = 0.037$, 0.341-fold) expression in LIN28 positive group was lower than that in LIN28 negative group of the patients. No significant associations were, however, detected between LIN28 immunoreactivity and other *let-7* family members in breast carcinoma cells. There were also no significant correlations between LIN28B immunoreactivity and the expression levels of *let-7* family in breast carcinoma cells (data not present).

4. Discussion

A possible interference of LIN28 towards *let-7* maturation process has been reported both in developmental stages and various human malignancies. In breast cancer, *let-7* miRNA deregulation was demonstrated *in silico*, *in vitro*, and *in vivo*, but the biological roles of LIN28 were not elucidated in these experiments [16,21,22]. In particular, *let-7* miRNAs have been demonstrated to silence multiple oncogenes such as c-Myc, RAS, and HMGA2 [23–25]. LIN28 is considered to reactivate these oncogenes, and to induce aggressive tumorigenesis through an inhibition of *let-7* precursor processing [8]. In this study, we firstly demonstrated notable interactions between LIN28 and hormone receptors in addition to reduction of *let-7* miRNA expression by LIN28 in breast carcinomas. Results of our present study, especially the significant correlation between LIN28 and ERα and Ki-67 status, suggest that LIN28 is a potential regulator of ER expression and induces estrogen dependent cell proliferation in breast carcinomas. LIN28 cannot be directly regulated by ERα as there is no ERα binding site [26]. However, previous studies have suggested that *let-7* can inhibit ERα expression [27]. Therefore, ERα may be induced by LIN28 through the down-regulation of *let-7* expression in breast carcinoma cells but it awaits further investigations for clarification. It has already been shown in ovarian cancer that high LIN28 status corresponds to increased Ki-67 expression and poor prognosis [12] as we have observed a similar pattern in Ki-67 status in this study. Taken together, results of these findings all indicate that high LIN28 levels in breast cancer may result in estrogen activation by suppressing *let-7* miRNA activities in carcinoma cells.

The roles of LIN28 and LIN28B are considered to be homogeneous in various tumorigenesis [9], but their details remain unknown. Results of several studies indicated that LIN28B was associated with an aggressive biological behavior in several human malignancies [28,29]. For instance, Viswanathan et al. reported that an activation of LIN28B may be associated with rare amplification or translocation of various oncogenes [30]. When LIN28B was over-expressed in colon cancer, the rate of cellular proliferation process in carcinoma cells was elevated, which then often resulted in metastasis and aggressive tumorigenesis [31]. In ovarian cancer, higher expression of LIN28B seemed to link with poor prognosis of the patients possibly via mediation of insulin-like growth factor-II [12]. To clarify precise roles of both LIN28 and LIN28B in biological behavior of breast cancer patients, further investigations are required including analysis of prognosis and recurrence rate.

In our present study, LIN28 was inversely correlated with only two members of *let-7* family, *let-7d* and *let-7f*. It has been shown that LIN28 inhibits *let-7* miRNA biogenesis at a post-transcriptional level, though in the absence of LIN28 both hnRNP A1 and KSRP can specifically target *let-7a* for its down-regulation [32]. This suggests that LIN28 is not necessarily the only regulatory candidate of *let-7* family, and these findings suggest that the regulation of *let-7* miRNA expressions may be intricate in biological behavior of breast cancer patients.

Estrogens are well-known to play pivotal roles in the great majority of breast carcinomas but in post-menopausal females and males, synthesis of estrogen is largely derived from intratumoral aromatase, an enzyme which converts androgen to estrogen [33]. Barh et al. studied multiple roles of *let-7* family in various human tumors, and reported that *let-7* may facilitate inactivation of aromatase by target scan analysis [34]. Therefore, the statistically significant correlation detected between LIN28 and ER in our data may be postulated in this context. In particular, an upstream repression of *let-7* (especially *let-7f*) by LIN28 could restore aromatase activity, which then precedes estrogen biogenesis, and subsequently synthesized estrogens may result in down-stream ER expression in these breast carcinoma cells.

A number of studies have shown that the inhibition of *let-7* miRNA precursor resulted in promotion of various oncogenic activity [3–6]. Results of our present study also demonstrated that the status of LIN28 may influence the prognosis of patients with estrogen-dependent breast carcinomas. By summing up previous data and our study, it is possible that LIN28 facilitates down-regulation of *let-7* miRNA in breast malignancy, particularly *let-7f* precursor [11]. From this, we can reasonably hypothesize a blockage of *let-7* maturation process by LIN28 at post-transcriptional level will increase intratumoral estrogen synthesis via aromatase reactivation in human breast cancer tissues.

Conflicts of interest

The authors have no conflicts of interest in this manuscript.

Acknowledgements

We thank Katsuhiko Ono (Department of Pathology, Tohoku University School of Medicine, Sendai, Japan) for skillful technical assistance and Keely McNamara (Department of Pathology, Tohoku University School of Medicine, Sendai, Japan) for skillful editing.

References

[1] S. Roush, F.J. Slack, The *let-7* family of microRNAs, Trends Cell Biol. 18 (10) (2008) 505–516.
[2] W. Filipowicz, S.N. Bhattacharyya, N. Sonenberg, Mechanisms of post-transcriptional regulation by microRNAs: are the answers in sight? Nat. Rev. Genet. 9 (2008) 102–114.
[3] M.S. Kumar, J. Lu, K.L. Mercer, et al., Impaired microRNA processing enhances cellular transformation and tumorigenesis, Nat. Genet. 39 (2007) 673–677.
[4] Y.S. Lee, A. Dutta, The tumor suppressor microRNA *let-7* represses the HMGA2 oncogene, Genes Dev. 21 (9) (2007) 1025–1030.
[5] S.M. Johnson, H. Grosshans, J. Shingara, et al., RAS is regulated by the *let-7* MicroRNA family, Cell 120 (5) (2005) 635–647.
[6] J. Schultz, P. Lorenz, G. Gross, et al., MicroRNA *let-7*b targets important cell cycle molecules in malignant melanoma cells and interferes with anchorage-independent growth, Cell Res. 18 (2008) 549–557.
[7] J. Takamizawa, H. Konishi, K. Yanagisawa, et al., Reduced expression of the *let-7* microRNAs in human lung cancers in association with shortened postoperative survival, Cancer Res. 64 (2004) 3753–3756.
[8] S.R. Viswanathan, G.Q. Daley, Lin28: a microRNA regulator with a macro role, Cell 140 (4) (2010) 445–449.
[9] S.R. Viswanathan, G.Q. Daley, R.I. Gregory, Selective blockage of microRNA processing by Lin28, Science 320 (5872) (2008) 97–100.
[10] J.A. Thompson, J. Itskovitz-Eldor, S.S. Shapiro, et al., Embryonic stem cell lines derived from human blastocytes, Science 282 (5391) (1998) 1145–1147.
[11] E. Balzer, C. Heine, Q. Jiang, V.M. Lee, E.G. Moss, LIN28 alters cell fate succession and acts independently of *let-7* microRNA during neurogliogenesis in vitro, Development 137 (2010) 891–900.
[12] A. Rybak, H. Fuchs, L. Smirnova, et al., A feedback loop comprising lin-28 and *let-7* controls pre-*let-7* maturation during neural stem-cell commitment, Nat. Cell Biol. 10 (2008) 987–993.
[13] M.A. Newman, J.M. Thomson, S.M. Hammond, Lin-28 interaction with the let-7 precursor loop mediates regulated microRNA processing, RNA 14 (2008) 1539–1549.
[14] L. Lu, D. Katsaros, K. Shaverdashvili, et al., Pluripotent factor lin28 and its homologue line28b in epithelial ovarian cancer and their associations with disease outcomes and expression of let-7a and IGF-II, Eur. J. Cancer 45 (12) (2009) 2212–2218.
[15] K. Inamura, Y. Togashi, K. Nomura, et al., *let-7* microRNA expression is reduced in bronchioloalalveoler carcinoma, a non-invasive carcinoma, and is not correlated with prognosis, Lung Cancer 58 (3) (2007) 392–396.

Please cite this article in press as: M. Sakurai, et al., LIN28: A regulator of tumor-suppressing activity of *let-7* microRNA in human breast cancer, J. Steroid Biochem. Mol. Biol. (2011), doi:10.1016/j.jsbmb.2011.10.007

[16] F. Yu, H. Yao, P. Zhu, et al., *Let-7* regulates self renewal and tumorigenicity of breast cancer cells, Cell 131 (2007) 1109–1123.
[17] A.J.M. Gillis, H. Stoop, K. Biermann, et al., Expression and interdependencies of pluripotency factors LIN28, OCT3/4, NANOG and SOX2 in human testicular germ cells and tumors of the testis, Int. J. Androl. 34 (4pt2) (2011) e160–e174.
[18] S. Hata, Y. Miki, F. Fujishima, et al., Cytochrome 3A and 2E1 in human liver tissue: individual variations among normal Japanese subjects, Life Sci. 86 (2010) 393–401.
[19] T. Suzuki, T. Nakata, Y. Miki, et al., Estrogen sulfotransferase and steroid sulfatase in human breast carcinoma, Can. Res. 63 (2003) 2762–2770.
[20] C. Schoroder, U. Schumacher, V. Muller, et al., The transcription factor Fra-2 promotes mammary tumor progression by changing the adhesive properties of breast cancer cells, Eur. J. Cancer 46 (2010) 1650–1660.
[21] D. Barh, S. Parida, B.P. Parida, G. Viswanathan, *Let-7*, mir-125, mir-205, and mir-296 are prospective therapeutic agents in breast cancer molecular medicine, Gene Ther. Mol. Biol. 12 (2008) 189–206.
[22] L.F. Sempere, M. Christensen, A. Silahtaroglu, et al., Altered microRNA expression confined to specific epithelial cell sub-populations in breast cancer, Cancer Res. 67 (2007) 11612–11620.
[23] A. Esquela-Kerscher, F.J. Slack, Oncomirs-microRNAs with a role in cancer, Nat. Rev. Can. 6 (2006) 259–269.
[24] C.D. Johnson, A. Esquela-Kerscher, G. Stefani, et al., The *let-7* microRNA represses cell proliferation pathways in human cells, Can. Res. 67 (2007) 7713–7722.
[25] M.V. Iorio, M. Ferracin, C.G. Liu, et al., MicroRNA gene expression deregulation in human breast cancer, Can. Res. 65 (16) (2005) 7065–7070.
[26] P. Bhat-Nakshatri, G. Wang, N.R. Collons, et al., Estradiol-regulated microRNAs control estradiol response in breast cancer cells, Nucleic Acids Res. 37 (14) (2009) 4850–4861.
[27] Y. Zhao, C. Deng, J. Wang, et al., *Let-7* family miRNAs regulate estrogen receptor alpha signaling in estrogen receptor positive breast cancer, Breast Cancer Res. Treat. 127 (2011) 69–80.
[28] T.C. Chang, L.R. Zeitels, H.W. Hwang, et al., Lin-28B transactivation is necessary for Myc-mediated *let-7* repression and proliferation, Proc. Natl. Acad. Sci. U.S.A. 106 (9) (2009) 3384–3389.
[29] Y. Guo, Y. Chen, H. Ito, et al., Identification and characterization of lin-28 homolog B (LIN28B) in human hepatocellular carcinoma, Gene 384 (2006) 51–61.
[30] S.R. Viswanathan, J.T. Powers, W. Einhorn, et al., LIN28 promotes transformation and is associated with advanced human malignancies, Nat. Genet. 41 (7) (2009) 843–848.
[31] C. King, M. Cuatrecasas, A. Castells, et al., Lin28b promotes colon cancer progression and metastasis, Can. Res. 71 (12) (2011) 4260–4268.
[32] G. Michlewski, J. Caceres, Antagonistic role of hnRNP A1 and KSRP in the regulation of *let-7*a biogenesis, Nat. Struct. Mol. Biol. 17 (8) (2010) 1011–1018.
[33] T. Suzuki, Y. Miki, Y. Nakamura, et al., Sex steroid-producing enzymes in human breast cancer, Endocr. Relat. Cancer 12 (2005) 701–720.
[34] D. Barh, R. Malhotra, B. Ravi, P. Sindhurani, MicroRNA *let-7*: an emerging next-generation cancer therapeutic, Curr. Oncol. 17 (1) (2010) 70–80.

Please cite this article in press as: M. Sakurai, et al., LIN28: A regulator of tumor-suppressing activity of *let-7* microRNA in human breast cancer, J. Steroid Biochem. Mol. Biol. (2011), doi:10.1016/j.jsbmb.2011.10.007

Cancer Science
The official journal of the Japanese Cancer Association JCA

Retrospective analysis of mammographic findings for Japanese women: A potential predictor for breast malignancies

Kentaro Tamaki,[1,2,3,4] Takanori Ishida,[2] Minoru Miyashita,[2] Masakazu Amari,[2] Noriaki Ohuchi,[2] Kano Uehara,[1] Yoshihiko Kamada,[1] Nobumitsu Tamaki[4] and Hironobu Sasano[3]

[1]Department of Breast Surgery, Nahanishi Clinic, Okinawa; [2]Department of Surgical Oncology, Tohoku University Graduate School of Medicine, Miyagi; [3]Department of Pathology, Tohoku University Hospital, Miyagi, Japan

(Received October 14, 2011/Revised November 14, 2011/Accepted November 20, 2011/Accepted manuscript online November 30, 2011/Article first published online December 28, 2011)

This purpose of this study was to retrospectively stratify the risks of malignancy according to the mammographic characteristics of Japanese women. We studied the mammographic findings of 1267 Japanese women. We characterized malignant phenotypes according to mass shape, margin and mass density, and by shape and distribution of calcified foci, and to obtain possible predictors for malignancies according to age groups. Lobular and irregular mass shape, no circumscribed margin and higher density turned out to be more powerful predictors for malignancy than other radiological factors ($P < 0.001$, respectively). The ratio of the cases detected as a mass in those between 21 and 49 years was lower than that of other age groups. In addition, the presence of calcifications and no mammographic abnormalities were the most powerful predictors for malignancies in the young age groups ($P < 0.001$, respectively). The peak age of breast cancer is between 40 and 49 years in Japan. In the present study, subtle differences were found in the mammographic results for young and old women, in contrast to those of women in the USA and Europe. The results of this study might enable more accurate prediction of biological behavior of the breast lesions in Japanese women. (*Cancer Sci* 2012; 103: 472–476)

The incidence of breast cancer continues to increase worldwide.[1] Morbidity and death due to breast cancer are lower in Japan than in the USA and Europe, but their rates have been markedly increased in this decade.[2] The effectiveness of screening mammography in reducing death from breast cancer has been established in both the USA, Europe and Japan.[3] Worldwide, millions of mammographic examinations are performed each year, and mammography has become the gold standard for detecting breast disorders. It is important to continue to increase the mammographic screening ratio in order to reduce breast cancer deaths.

The American College of Radiology (ACR) has developed the Breast Imaging Reporting and Data System (BI-RADS) to standardize mammographic reporting, to improve communication with clinicians, to reduce confusion regarding mammographic findings, to aid research and to facilitate outcomes monitoring.[4] The use of BI-RADS lexicon is increasing not only in the North American continent but also worldwide.[5] However, some publications have raised the issue of observer variability of interpretation of the lexicon, and have even questioned the expressiveness of the BI-RADS system.[6,7] Some published studies propose classifications of features for the assignment of findings to the various BI-RADS categories.[6,7]

Some published reports suggest possible differences in the biological characteristics of breast cancer between women in the USA and Europe and Japanese women.[8] A striking difference is that the peak age for breast cancer is between 40 and 50 years in Japan, whereas the peak age in the USA and Europe is between 60 and 70 years.[8] We have observed that the mammographic findings for Japanese women do not exactly correspond to those defined in BI-RADS lexicon. The dense parenchyma in women before menopause can obscure tumor shadows, which results in the lower sensitivity of mammography screening in women 40–49 years of age.[9] The purpose of the present study was to retrospectively stratify the risk of malignancy according to mammographic characteristics of Japanese women.

Materials and Methods

Patients. This is a retrospective study. We examined mammographical findings of 1267 Japanese women (707 malignant and 560 benign breast diseases) who underwent needle biopsies or surgical resection at the Tohoku University Hospital. We received informed consent from all patients and the protocol for this study was approved by the Ethics Committee at Tohoku University Graduate School of Medicine. The median age of the patients was 52 years (range, 21–89 years). The numbers of biopsy or surgical resection cases were: 151 for 21–39 years, 393 for 40–49 years, 355 for 50–59 years, 215 for 60–69 years and 153 for 70–89 years. The numbers of malignant cases were: 56 for 20–39 years, 205 for 40–49 years, 175 for 50–59 years, 147 for 60–69 years and 124 for 70–89 years. The criteria for performing a biopsy were BI-RADS assessment categories of mammography and ultrasound category 4 or more.

Imaging and evaluation. All mammographic examinations were performed with dedicated machines. Analog mammographic examinations were performed with one unit (MAMMOMAT 3000 Nova; Siemens AG, Erlangen, Germany) and using a screen-film technique (Min-R 2000 Min-R EV; Kodak Health Imaging, Rochester, NY, USA). Digital mammograms were acquired using a system with an amorphous selenium DirectRay digital detector (LOARD Selenia; Hologic, Waltham, MA, USA). The system was connected to a viewing monitor (MammoRead; TOYO Corporation, Tokyo, Japan).

We first examined the correlation between mammographic findings and the ratio of malignant cases. Two of the authors independently evaluated mammographic findings. These two investigators were blinded to the clinical outcome of the patients. The presence of mass, calcification and the other findings, including architectural distortion, focal asymmetric density and asymmetric breast tissue (ABT) were each recorded. As for mass, shape was tentatively classified as round, oval, lobular or irregular. Margin was classified as circumscribed, microlobulated, indistinct or spiculated. Density was classified into higher,

[4]To whom correspondence should be addressed.
E-mail: nahanisikenta@yahoo.co.jp

doi: 10.1111/j.1349-7006.2011.02169.x

equivalent or lower. Shape of calcification was tentatively classified as punctuate, amorphous, pleomorphic or linear. Distribution was classified as diffuse, grouped or segmental. We classified FAD and ABT into those with or without architectural distortion. We first examined the correlation between mammographic findings and the ratio of malignant cases. We then examined the ratio of malignant cases according to mammographic findings. We devised classification system for predicting. In addition, we attempted to obtain possible predictors for malignancies according to age groups: 21–39, 40–49, 50–59, 60–69 and 70–89 years. If there were two or more findings in a mammography, we determined the priority for mammographic findings as follows: mass, calcification, other findings including architectural distortion, FAD and ABT, and no mammographic abnormality, and recorded a prior finding as a possible predictor for malignancy.

Statistical analysis. Statistical analyses were performed using StatMate IV for Windows (ATMS, Tokyo, Japan). Results were considered significant at $P < 0.05$.

Results

Sensitivity, specificity and PPV by age groups. Of the 1040 cases with mammographic findings, 656 were malignant and 384 were benign, whereas 51 of the 227 cases without any mammographic findings were malignant. Sensitivity, specificity and positive predictive value were 92.8, 31.4 and 63.1%, respectively. In addition, sensitivity, specificity and PPV by age groups were: 87.5, 40.0 and 46.2% for 21–39 years; 86.8, 35.2 and 51.5% for 40–49 years; 96.1, 29.3 and 66.6% for 50–59 years, 96.6%, 17.6 and 71.7% for 60–69 years; and 93.5, 31.0 and 85.3% for 70–89 years, respectively.

Correlation between mammographic findings and ratio of malignant cases. The ratio of malignant cases according to the mass shape were 46.7% (28/60) of round, 45.1% (23/51) of oval, 83.3% (62/74) of lobular and 94.9% (131/138) of irregular lesions, respectively (Fig. 1A). There were statistically significant differences between round or oval and lobular or irregular shape ($P < 0.001$, respectively). The ratio of malignant cases according to the margin were 19.3% (11/57) of circumscribed, 75.5% (74/98) of microlobulated, 87.3% (62/71) of indistinct and 100% (97/97) of spiculated margin, respectively (Fig. 1B). There were statistically significant differences between circumscribed and the other characteristics, and microlobulated and spiculated margin ($P < 0.001$, respectively). The ratios of malignant cases according to mass density were 81.7% (210/257) of higher, 55.9% (33/59) of equivalent and 14.3% (1/7) of lower mass density, respectively (Fig. 1C). There were statistically significant differences between higher and equivalent or lower mass density ($P < 0.001$). The ratios of malignant cases according to calcification type were 28.1% (25/89) of punctuate, 48.3% (129/267) of amorphous, 88.4% (137/155) of pleomorphic and 100% (20/20) of linear type, respectively (Fig. 2A). There were statistically significant differences between punctuate or amorphous and any calcification shapes ($P = 0.001$ for between punctuate and amorphous, $P < 0.001$ for the other combinations). The ratios of malignant cases according to distribution of calcification were 16.7% (1/6) of diffuse, 53.1% (146/275) of grouped and 65.6% (164/250) of segmental (Fig. 2B). There were statistically significant differences between segmental and diffuse or grouped cases ($P = 0.041$ and $P = 0.005$, respectively).

Classifications for predicting malignancies. We attempted to devise a classification system predicting malignancies (Table 1). The masses with spiculated or microlobulated margins, and the masses with lobular or irregular mass shapes and indistinct margins turned out to be more powerful predictors of malignancies than the other radiological factors ($P < 0.001$). In contrast, the masses with circumscribed margins and equivalent or lower mass densities were less powerful predictors of malignancies ($P = 0.154$).

Mammographic findings of all the cases by age groups. Mammographic findings of all cases by age group are summarized in Figure 3A. The ratios of the cases detected as a mass were 18.5% for 21–39 years, 16.8% for 40–49 years, 25.4% for 50–59 years, 31.6% for 60–69 years and 46.4% for 70–89 years, respectively. There were statistically significant differences between 21 and 39 and 60–69 ($P = 0.007$) or 70–89 years ($P < 0.001$), 40–49 and 50–59 years ($P = 0.005$), 60–69 ($P < 0.001$) or 70–89 years ($P < 0.001$), 50–59 and 70–89 years ($P < 0.001$), and 60–69 and 70–89 years ($P = 0.006$). The ratios of calcification were 29.8% for 21–39 years, 41.7% for 40–49 years, 41.4% for 50–59 years, 39.5% for 60–69 years and 24.8% for 70–89 years, respectively. There were statistically significant differences between 20 and 39 and 40–49 ($P = 0.014$) or 50–59 years ($P = 0.021$), 40–49 and 70–89 years ($P < 0.001$), 50–59 and 70–89 years ($P < 0.001$), and 60–69 and 70–89 years ($P = 0.005$). The ratios of the other findings, including architectural distortion, FAD and ABT were 21.9% for 21–39 years, 16.3% for 40–49 years, 19.7% for 50–59 years, 20.9% for 60–69 years and 17.6% for 70–89 years, respectively. There were no statistically significant differences

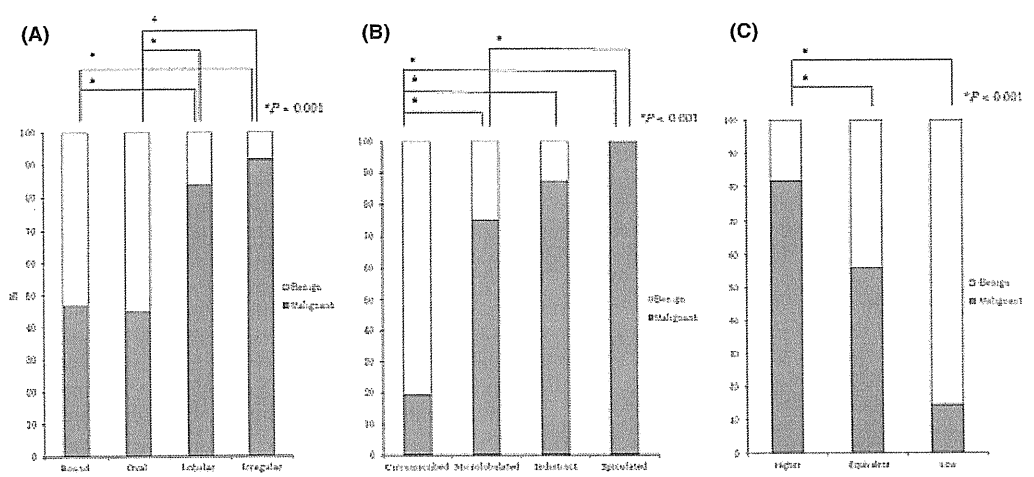

Fig. 1. Correlation between mammographic findings of masses and malignant ratio: (A) mass shape, (B) margin and (C) mass density.

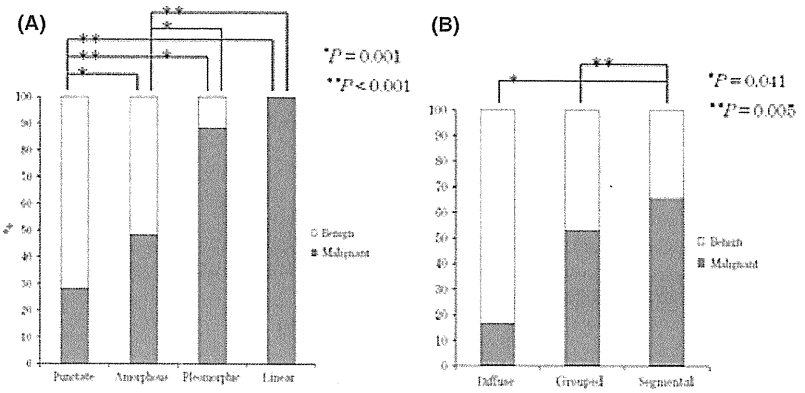

Fig. 2. Correlation between mammographic findings of calcifications and malignant ratio: (A) characteristics of calcification and (B) distribution.

Table 1. Classifications for predicting malignancies

	Malignant ratio (%)		Mammographic findings	Total number	No. malignancies	Ratio of malignant cases (%)	*P*-value	Odds ratio
Class I	0–20	Mass	Any mass shape-circumscribed-equivalent or lower	25	2	8.0	0.154	0.30
		Calcification	Punctate-diffuse or grouped	42	7	16.7	0.525	0.69
Class II	20–40	Mass	Round-circumscribed-higher-with calcification	19	5	26.3	0.921	1.23
			Oval-circumscribed-higher	12	3	25.0	0.881	1.15
			Oval-microlobulated-equivalent	8	3	37.5	0.572	2.07
		Calcification	Punctate-segmental	28	6	21.4	0.907	0.94
			Amorphous-diffuse or grouped	106	30	28.3	0.308	1.36
Class III	40–60	Mass	Round-indistinct-higher	4	2	50.0	0.485	3.45
			Lobular-microlobulated or indistinct-equivalent	6	3	50.0	0.277	3.45
		Calcification	Punctate-grouped-with FAD	9	5	55.6	0.589	4.31
			Amorphous-segmental	86	37	43.0	<0.001	2.61
		FAD	Without distortion	123	50	40.7	<0.001	2.36
Class IV	60–80	Mass	Irregular, round or lobular-microlobulated-higher	62	46	74.2	<0.001	9.92
		Calcification	Punctate-segmental-with FAD	6	4	66.7	0.420	6.90
			Amorphous-grouped or segmental-with FAD	53	41	77.4	<0.001	11.79
			Pleomorphic-grouped	43	33	76.7	<0.001	11.39
		ABT	Without distortion	5	4	80.0	0.014	13.80
Class V	80–100	Mass	Any mass shape-spiculated-any density	100	100	100.0	<0.001	–
			Any mass shape-microlobulated-any density-with calcification	18	17	94.4	<0.001	58.67
			Lobular or irregular-obscured or indistinct-any findings	64	58	90.6	<0.001	33.36
		Calcification	Pleomorphic-grouped or segmental with FAD	32	29	90.6	<0.001	33.36
			Pleomorphic-segmental	58	53	91.4	<0.001	36.58
			Linear-any distribution	16	16	100.0	<0.001	–
		FAD	With distortion	90	77	85.6	<0.001	20.44
		ABT	With distortion	20	20	100.0	<0.001	–

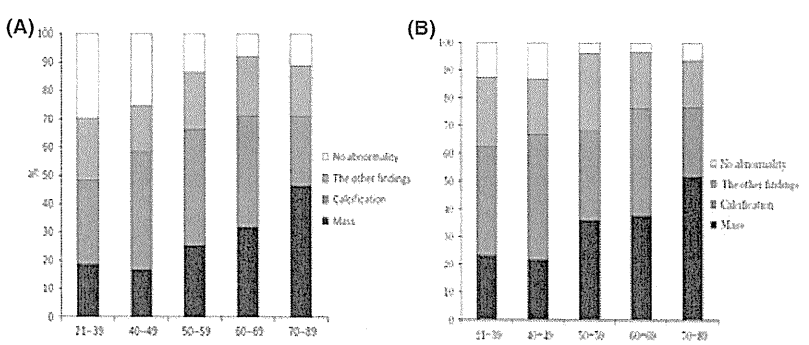

Fig. 3. The ratio of mammographic findings by age groups: (A) mammographic findings of all cases by age groups and (B) mammographic findings of malignant cases by age groups.

doi: 10.1111/j.1349-7006.2011.02169.x

among age groups. The ratios of the cases without mammographic abnormalities were 29.8% for 21–39 years, 25.4% for 40–49 years, 13.8% for 50–59 years, 7.9% for 60–69 years and 11.1% for 70–89 years, respectively. There were statistically significant differences between 21 and 39 and 50–59 ($P < 0.001$), 60–69 ($P < 0.001$) or 70–89 years years ($P < 0.001$), 40–49 and 50–59 ($P < 0.001$), 60–69 ($P < 0.001$) or 70–89 years ($P < 0.001$), and 50–59 and 60–69 years ($P = 0.046$).

Mammographic findings of malignant cases by age groups. Mammographic findings of malignant cases by age group are summarized in Figure 3B. The ratios of the cases detected as a mass were 23.2% for 21–39 years, 21.7% for 40–49 years, 36.1% for 50–59 years, 37.4% for 60–69 years and 51.6% for 70–89 years, respectively. There were statistically significant differences between 21 and 39 and 70–89 years ($P < 0.001$), 40–49 and 50–59 ($P = 0.003$), 60–69 ($P = 0.003$) or 70–89 years ($P < 0.001$), 50–59 and 70–89 years ($P = 0.008$), and 60–69 and 70–89 years ($P = 0.026$). The ratios of calcification were 39.3% for 21–39 years, 45.1% for 40–49 years, 35.1% for 50–59 years, 38.8% for 60–69 years and 25.0% for 70–89 years, respectively. The only statistically significant differences ware between 40 and 49 and 70–89 years ($P < 0.001$). The ratios of the other findings including architectural distortion, FAD and ABT were 25.0% for 21–39 years, 19.4% for 40–49 years, 24.9% for 50–59 years, 20.4% for 60–69 years and 22.1% for 70–89 years. There were statistically significant differences between 50 and 59 and 70–89 years ($P = 0.046$). The ratios of the cases without mammographic abnormalities were 12.5% for 21–39 years, 13.1% for 40–49 years, 3.9% for 50–59 years, 3.4% for 60–69 years and 6.5% for 70–89 years, respectively. There were statistically significant differences between 21 and 39 and 50–59 ($P = 0.034$) or 60–69 years ($P = 0.034$), and 40–49 and 50–59 ($P = 0.002$) or 60–69 years ($P = 0.004$).

Mammographic predictors for malignancy by age groups. The distinctive mammographic predictors for malignancy by age group are summarized in Table 2. The masses not only spiculated but also with microlobulated and indistinct margins turned out to be powerful predictors for malignancies in the groups of 50–59 years and above (Table 2).

Discussion

The BI-RADS lexicon was created and has evolved to help capture predictive mammographic descriptors in a standardized manner in the USA and Europe.[4,10] Various biological features of breast cancer have been found to be different between women in the USA and Europe and Japanese women.[8,11] Mammographic findings of Japanese women do not exactly correspond to those defined in BI-RADS lexicon for women in the USA and Europe.

The results of this study demonstrate that lobular and irregular mass shape, no circumscribed margin and higher density are more powerful predictors of malignancy than the other findings with statistical significance. As for calcification, a statistically significant difference was detected between necrotic and secretary calcification. FAD combined with architectural distortion represented a high malignant ratio of up to 80%. These results were similar to those in the BI-RADS lexicon.

Table 2. Mammographic predictors for malignancy by age groups

Years		Mammographic findings	Total number	No. malignancies	Ratio of malignant cases (%)	*P*-value	Odds ratio
21–39	Mass	Irregular-spiculated: with calcification	4	4	100.0	0.001	–
	Calcification	Amorphous-segmental-with FAD	4	4	100.0	0.001	–
		Pleomorphic-any distribution	11	9	81.8	<0.001	15.53
	FAD	With distortion	11	8	72.7	<0.001	14.1
40–49	Mass	Lobular-indistinct or spiculated-high	5	5	100.0	0.001	–
		Irregular-indistinct-high	10	8	80.0	<0.001	13.8
		Irregular-spiculated-any density	13	13	100.0	<0.001	–
	Calcification	Amorphous-segmental	52	26	50.0	0.001	3.35
		Pleomorphic-any distribution	37	35	94.6	<0.001	58.59
		Linear-segmental	4	4	100.0	0.004	–
	FAD	With distortion	23	19	82.6	<0.001	15.9
	ABT	With distortion	4	4	100.0	0.004	–
50–59	Mass	Round-indistinct or microlobulated-equivalent or high	6	6	100.0	<0.001	–
		Oval-microlobulated-high	8	6	75.0	0.002	15.35
		Lobular-indistinct or microlobulated-high	14	13	92.9	<0.001	44.86
		Irregular-indistinct, obscured or spiculated	43	43	100.0	<0.001	–
	Calcification	Amorphous-grouped-with FAD	8	8	100.0	<0.001	–
		Amorphous-segmental	27	14	51.9	0.002	3.72
		Pleomorphic-any distribution	43	33	76.7	<0.001	11.39
	FAD	With or without distortion	63	44	69.8	<0.001	7.99
	ABT	With distortion	7	7	100.0	<0.001	–
60–69	Mass	Round-circumscribed or microlobulated-high	6	6	100.0	0.012	–
		Lobular-microlobulated or indistinct-any density	11	10	90.9	<0.001	34.51
		Irregular-any periphery-any density	31	31	100.0	<0.001	–
	Calcification	Amorphous-segmental-with FAD	5	5	100.0	0.025	–
		Pleomorphic-any distribution	28	26	92.9	<0.001	31.2
		Linear-any distribution	5	5	100.0	0.045	–
	FAD	With distortion	19	17	89.5	<0.001	20.4
	ABT	With or without distortion	4	4	100.0	0.045	–
70–89	Mass	Lobular or irregular, any periphery, any density	52	49	94.2	<0.001	56.37
	Calcification	Pleomorphic, any distribution	14	13	92.9	0.013	16.25

However, the striking difference between Japanese and the USA and Europe breast cancer patients is that the peak age for breast cancer was between 40 and 50 years in the Japan, whereas the peak age in the USA and Europe was between 60 and 70 years.[8] The results of our present study reveals that the peak age of breast cancer was 40 years. There were subtle differences in mammographic findings between young and old women, which are different from those of women in the USA and Europe. Previous studies have demonstrated that mass is the more powerful predictor in women in the USA and Europe.[12,13] However, the results in the present study demonstrate that the ratio of the cases detected as a mass between 21 and 49 years was lower than that of the other age groups. In addition, the masses that were spiculated and had microlobulated and indistinct margins turned out to be powerful predictors for malignancies in those of 50 years and above, whereas only limited masses were predictors for those under 49 years old. Therefore, the presence of a mammographic mass is not necessarily the most powerful predictor for malignancy in Japanese women.

The results of the present study also demonstrated that 7.2% (51/707) of malignant cases had mammographic abnormalities. In addition, the ratios of malignant cases in those of 20, 30 and 40 years without mammographic abnormalities were statistically higher than the ratios of the other age groups. There was dense parenchyma in women before menopause. A previous study demonstrated that the percentage of extremely dense and dense breast were 76.3% of 40 years, 51.5% of 50 years and 17.6% of 60 years in Japanese breast cancer cases, respectively.[9] Breast masses are indicated by their density in the mammography. In addition, the mass findings are often hidden in a dense breast. Previous study has demonstrated that screening mammography is effective for women aged 50 years and over to detect malignancy, whereas the effectiveness for women under 50 years has not been proven.[3] Ohuchi *et al.*[14] suggested that screening mammography alone for Japanese women aged 40 years and over is insufficient. For the purpose of complementing this weakness of mammography, the effectiveness of ultrasound screening for women aged 40 years and over has been evaluated in relation to detecting and reducing death as a result of breast cancer in Japan.[14]

In the present study, we attempted to establish mammographic criteria for Japanese women for predicting breast malignancy. We examined the mammographic characteristics according to age groups. Lobular and irregular mass shape, no circumscribed margin and higher density turned out to be more powerful predictors for malignancy than other radiological factors. In addition, the ratio of the cases detected as a mass between 21 and 49 years was lower than that for other age groups. The presence of calcifications and no mammographic abnormalities was one of the most powerful predictors for malignancies in the young age groups. However, this study was retrospective and took place in a single institute. Therefore, it is probable that further investigation not only with Japanese women but also with other Asian women will confirm the new mammographic criteria. The results of this study might enable more accurate prediction of the biological behavior of the breast lesions in Japanese women.

Acknowledgments

This work was supported in part by a Grant-in-Aid from the Kurokawa Cancer Research Foundation.

Disclosure Statement

The authors have no conflict of interest.

References

1 Sutela A, Vanninen R, Sudah M *et al.* Surgical specimen can be replaced by core samples in assessment of ER, PR and HER-2 for invasive breast cancer. *Acta Oncol* 2008; **47**: 38–46.
2 Endo T. International exchange activities with East Japanese countries through mammography. *Breast Cancer* 2008; **16**: 10–17.
3 Kawai M, Kuriyama S, Suzuki A *et al.* Effect of screening mammography on breast cancer survival in comparison to other detection methods: a retrospective cohort study. *Cancer Sci* 2009; **100**: 1479–84.
4 American College of Radiology. *Breast imaging reporting and data system (BI-RADS)*, 4th edn. Reston, VA: American College of Radiology, 2003.
5 Stines J. BI-RADS: use in the French radiologic community. How to overcome with some difficulties. *Eur J Radiol* 2007; **61**: 224–34.
6 Burnside ES, Ochsner JE, Fowler KJ *et al.* Use of microcalcification descriptors in BI-RADS 4th edition to stratify risk of malignancy. *Radiology* 2007; **242**: 388–95.
7 Berube M, Curpen B, Ugolini P *et al.* Level of suspicion of a mammographic lesion: use of features defined by BI-RADS lexicon and correlation with large-core breast biopsy. *Can Assoc Radiol J* 1998; **49**: 223–8.
8 Leong SP, Shen ZZ, Liu TJ *et al.* Is breast cancer the same disease in Japanese and Western countries? *World J Surg* 2010; **34**: 2308–24.
9 Suzuki A, Kuriyama S, Kawai M *et al.* Age-specific interval breast cancers in Japan: estimation of the proper sensitivity of screening using a population-based cancer registry. *Cancer Sci* 2008; **99**: 2264–7.
10 American College of Radiology. *Breast Imaging Reporting and Data System (BI-RADS)*. 4th edn. Reston, VA: American College of Radiology, 1998.
11 Hortobagyi GN, De la Garza Salazar J, Pritchard K *et al.* The global breast cancer burden: variations in epidemiology and survival. *Clin Breast Cancer* 2005; **6**: 391–401.
12 Piasso ED, Fajardo LL, Tsimikas J *et al.* Rate of insufficient samples for fine-needle aspiration for nonpalpable breast lesions in a multicentral clinical trial. *Cancer* 1998; **82**: 679–88.
13 Thurfjell MG, Lindgren A, Thurfjell E. Nonpalpable breast cancer: mammographic appearance as predictor of histologic type. *Radiology* 2002; **222**: 165–70.
14 Ohuchi N, Ishida T, Kawai M *et al.* Randomized controlled trial on effectiveness of ultrasonography screening for breast cancer in women aged 40–49 (J-START): research design. *Jpn J Clin Oncol* 2011; **41**: 275–7.

doi: 10.1111/j.1349-7006.2011.02169.x

Molecular and Cellular Endocrinology 350 (2012) 99–106

Contents lists available at SciVerse ScienceDirect

Molecular and Cellular Endocrinology

journal homepage: www.elsevier.com/locate/mce

Synergistic anti-tumor effects of RAD001 with MEK inhibitors in neuroendocrine tumors: A potential mechanism of therapeutic limitation of mTOR inhibitor

Shinya Iida, Yasuhiro Miki, Katsuhiko Ono, Jun-ichi Akahira, Yasuhiro Nakamura, Takashi Suzuki, Hironobu Sasano *

Department of Pathology, Tohoku University Graduate School of Medicine, Sendai, Japan

ARTICLE INFO

Article history:
Received 15 June 2011
Received in revised form 25 October 2011
Accepted 25 November 2011
Available online 8 December 2011

Keywords:
Neuroendocrine tumors
Mammalian target of rapamycin
Mitogen-activated protein kinase
Signal transduction

ABSTRACT

Mammalian target of rapamycin (mTOR) inhibitors have been clinically used as anticancer agents in several types of human malignancies including neuroendocrine tumor (NET) but the development of clinical resistances or their therapeutic limitations have been also reported. This clinical resistance has been proposed to be partly due to a compensatory activation of an mTOR upstream factor Akt and MEK/ERK pathway in NET cells but its details have not necessarily been reported. Therefore, in this study, we examined the effects of mTOR inhibitors on these activations and of the concomitant treatment of mTOR and MEK inhibitors in two NET cell lines, NCI-H727 and COLO320. We evaluated the effects of RAD001, mTOR inhibitor, and U0126, MEK inhibitor, on cell proliferation and migration of these cells. In addition, an alteration of the factors involved in Akt/mTOR and MEK/ERK pathways was also examined under administration of these agents. RAD001 and U0126 treatment significantly inhibited cell proliferation and their combined treatment synergistically decreased it in both cell lines. Additionally, these treatments above decreased the expression of cell cycle-related factors, suggestive of an involvement of cell cycle arrest in therapeutic effects. The combined treatment also inhibited the cell migration in NCI-H727 via the decrement of MMP2 and 9 in an additive manner. We demonstrated the potential synergistic/combined effects of inhibitors of mTOR and MEK on cell proliferation and migration. These results suggest the potential therapeutic efficacy of the combined therapy of mTOR and MEK inhibitors or a dual inhibitor for the treatment of NET patients.

1. Introduction

Mammalian target of rapamycin (mTOR) plays a pivotal role in the regulation of several cell functions such as cell proliferation, survival, translation and metabolism (Bjornsti and Houghton, 2004; Pouysségur et al., 2006; Wullschleger et al., 2006). mTOR is a central regulator in phosphatidylinositol 3-kinase (PI3K)/Akt/mTOR pathway under receptor tyrosine kinases (RTKs) and has been recently examined as a novel therapeutic target for human neoplasms including neuroendocrine tumor (NET) because this pathway is commonly over-activated in NET (Ciuffreda et al., 2010). In addition, we and other investigators also reported the association between the overactivation of this pathway and insulin-like growth factor-1 receptor (IGF-1R) or epidermal growth factor receptor (EGFR) in NET (Iida et al., 2010; von Wichert et al., 2000; Zutzmann et al., 2007).

mTOR is composed of two complexes, mTOR complex 1 (mTORC1) and mTORC2, in terms of the functional activity (Thomson et al., 2009). mTORC1 inhibitors, rapamycin and its analogues (rapalogs), have been considered to demonstrate immunosuppressive and antitumor activities through the following mechanisms: rapalogs first bind to immunophilin FK506-binding protein 12 (FKBP12) and this complex subsequently binds to mTORC1, not to mTORC2, which results in an inhibition of downstream signaling pathways (Jayaraman and Marks, 1993; Loewith et al., 2002; Vilella-Bach et al., 1999). The detailed function of mTORC2 has not been well-characterized mainly because mTORC2 is insensitive to rapalogs and mTORC2-specific inhibitors are not still available at this juncture. Rapalogs, including CCI-779 (Wyeth), AP23573 (ARIAD Pharmaceuticals Inc.), and RAD001 (everolimus; Novartis AG), have been used in various clinical trials as an antitumor agent alone against various tumor types. For example, rapalogs demonstrated marked clinical therapeutic effects and relatively satisfactory safety profiles as a single agent in advanced renal cell carcinoma (Phase III) and mantle-cell lymphoma (Phase III) (Amato et al., 2009; Hess et al., 2009; Vilella-Bach et al., 1999). As for the patients with metastatic pancreatic

* Corresponding author. Address: Department of Pathology, Tohoku University Graduate School of Medicine, 2-1 Seiryo-machi, Aoba-ku, Sendai, Miyagi 980-8575, Japan. Tel.: +81 22 717 8050; fax: +81 22 717 8051.
E-mail address: hsasano@patholo2.med.tohoku.ac.jp (H. Sasano).

0303-7207/$ - see front matter © 2011 Elsevier Ireland Ltd. All rights reserved.
doi:10.1016/j.mce.2011.11.024

NET, Phase III clinical trials are also being carried out (Chan et al., 2010; Yao et al., 2011). It is, however, also true that results of these clinical trials employing this as a single agent or in combination with chemotherapeutic agents turned to be less successful than expected, which could limit its antitumor activity in clinical settings.

Recently, two potential mechanisms of the limitations or resistances to mTOR inhibition have been proposed. O'Reilly et al. (2006) reported that mTOR inhibition resulted in an activation of Akt, an upstream factor of mTOR, through upregulation of RTKs or of its substrates such as PDGFRs and IRS-1 (Hartley and Cooper, 2002; Zhang et al., 2007). Octreotide, which has been widely used for the treatment of NET patients, has been reported to decrease Akt phosphorylation (Charland et al., 2001; Theodoropoulou et al., 2006) and the effects of combination with rapalogs and octreotide were also evaluated against NET in both preclinical and clinical settings (Grozinsky-Glasberg et al., 2008; Moreno et al., 2008; Yao et al., 2008; Pavel et al., 2011). Results of these studies above all indicated that mTOR inhibitors were associated with significant antiproliferative activities but octreotide itself was not necessarily associated with sufficient antiproliferative effects as a single agent. Therefore, the clinical significance of additive effects of the combined treatment of mTOR inhibitors and octreotide has still remained in dispute.

The great majority of the studies exploring the limitation or resistance of antitumor effects of rapalogs studied their correlation with PI3K/Akt signaling pathway but several investigators reported that mTOR inhibition resulted in an activation of the MEK/ERK cascade through a PI3K-dependent feedback loop (Carracedo et al., 2008; Mi et al., 2009; Wang et al., 2008). In these studies, the combined treatment of both mTOR and MEK inhibitors improved the growth inhibitory effects of mTOR inhibition both *in vitro* and *in vivo* in various types of human malignancies. The dual inhibition of Ras/Raf/MEK/ERK and PI3K/Akt/mTOR pathways has also been reported as a potential anti-neoplastic therapy in glioma (Hjelmeland et al., 2007), prostate cancer (Kikade et al., 2008), melanoma (Lasithiotakis et al., 2008), thyroid cancer (Jin et al., 2009), pancreatic cancer (Chang et al., 2010) and glioblastoma (Sunayama et al., 2010). However, it is also true that the association between PI3K/Akt/mTOR and MEK/ERK pathways in NET cells has not been studied in details. Therefore, in this study, we hypothesized that the combined or synergistic effects of a dual inhibition of mTOR and MEK may result in a better therapeutic outcome in NET patients and evaluated this possibility using NET cell lines.

2. Materials and methods

2.1. Cell culture and reagents

NCI-H727, a human bronchial NET cell line, was purchased from the American Type Culture Collection (Manassas, VA, USA). COLO320-DM (COLO320) has been generally used as a human colon adenocarcinoma having neuroendocrine characteristics (Quinn et al., 1979) and we used this cell line in this study. This was purchased from The Health Science Research Resources Bank (Osaka, Japan). These cells were cultured in RPMI-1640 medium (Sigma Aldrich Co., St. Louis, MO, USA) containing 10% fetal bovine serum (FBS; Nichirei Co., Ltd., Tokyo, Japan). MEK inhibitor U0126 ethanolate (1,4-diamino-2,3-dicyano-1,4-bis[2-aminophenylthio]-butadiene) was purchased from Sigma Aldrich and RAD001 (everolimus) was kindly provided from Novartis AG (Basel, Switzerland). These reagents were dissolved in DMSO.

2.2. Antibodies

Primary antibodies employed in immunocytochemistry were as follows: anti-chromogranin A, anti-neuron specific enolase (NSE) and anti-synaptophysin (Dako, Glostrup, Denmark). For immunoblot analysis, the following antibodies were used (all from Cell Signaling Technology except where indicated): anti-Akt (#4685) and anti-phospho-Ser473-Akt (#4060), anti-mTOR (#2983) and anti-phospho-Ser2448-mTOR (#2971), anti-RpS6 (S6; #2217) and anti-phospho-Ser240/244 RpS6 (#2215), anti-4EBP1 (#9644) and anti-phospho-Thr70-4EBP1 (#9455), anti-p44/42 MAPK (ERK; #4695) and anti-phospho-Thr202/Tyr204-p44/42 MAPK (#4376), anti-Cyclin D1 (Dako Cytomation, Glostrup, Denmark), anti-Cyclin B1 (SantaCruz Biotechnology, Santa Cruz, CA) and anti-β-actin (Sigma Aldrich).

2.3. Immunocytochemistry

The cells were cultured in the 4-well slide (Nalge Nunc International) until reaching 80–90% confluence and then the slides were fixed with 10% formalin for 5 min at room temperature. Immunocytochemistry was performed as we previously reported (Iida et al., 2010). The cells were immunostained by a biotin–streptavidin method using Histofine kit (Nichirei Co., Ltd., Tokyo, Japan; chromogranin A and synaptophysin) and EnVision$^+$ method (Dako; NSE). The antigen–antibody complex was subsequently visualized with 3,3'-diaminobenzidine (DAB) solution (Dako Liquid DAB + Substrate System; Dako) and counterstained with hematoxylin.

2.4. Cell proliferation assay

The status of cell proliferation of NCI-H727 and COLO320 cells was determined using WST-8 [2-(2-methoxy-4-nitrophenyl)-3-(4-nitrophenyl)-5-(2,4-disulfophenyl)-2H-tetrazolium monosodium salt] method (Cell Counting Kit-8; Dojindo Inc., Kumamoto, Japan). The methods were based upon those which we previously reported (Iida et al., 2010).

2.5. Evaluation of combination index

In order to determine whether the combined effects were additive, synergistic or antagonistic, proliferation assay was conducted as follows: both RAD001 and U0126 were simultaneously administered at the ratio of 1:10 (NCI-H727) or 1:100 (COLO320) for 3 days. We analyzed the combination effects or "synergism" based upon the combination index (CI) method of Chou and Talalay (Chou and Talalay, 1984; Chou, 2006, 2010) using CalcuSyn software (version 2.0; Biosoft, Cambridge, UK). $CI < 1.0$ indicates synergism, $CI = 1.0$ indicates additivity and $CI > 1.0$ indicates antagonism.

2.6. Immunoblot analysis

Both NCI-H727 and COLO320 were treated with each single reagent or their combination conditions for adequate length of time and the total protein of the cells was extracted using PhosphoSafe™ Extraction Reagent (Biosciences Inc., Darmstadt, Germany). Following the measurement of protein concentration (Protein Assay Kit Wako: Wako), the total protein was individually subjected to SDS–PAGE (SuperSep™Ace: Wako). The proteins were then transferred onto Hybond P polyvinylidene difluoride membrane (GE Healthcare, Buckinghamshire, UK). The membranes were then blocked in 5% non-fat dry skim milk powder (Wako) for over 1 h at room temperature, and were then incubated with primary antibodies for 24–48 h at 4 °C using ImmunoShot (Cosmo Bio Co., Ltd., Tokyo, Japan). The working dilutions of the primary antibodies used in this study were summarized as follows: mTOR, Akt, S6, 4EBP1, ERK and β-actin, 1/1000; phosphorylated mTOR (p-mTOR), p-Akt, p-S6, p-4EBP1, p-ERK and Cyclin B1, 1/500; Cyclin D1, 1/250.

These antibody–protein complexes on the blots were detected using ECL-plus Western blotting detection reagents (GE Healthcare) following incubation with anti-mouse or anti-rabbit IgG horseradish peroxidase (GE Healthcare) at room temperature. The corresponding protein bands were subsequently visualized and analyzed using LAS-1000 cooled CCD-camera chemiluminescent image analyzer and Multi Gauge v3.1 software (both from Fuji Photo Film Co., Ltd., Tokyo, Japan), respectively.

2.7. Wound healing assay

We employed wound healing assay (Liang et al., 2007) in order to evaluate the *in vitro* migration of NCI-H727 cells. The confluent cell layer was scratched with a sterile plastic P-200 pipette tip. The cells migrated into these scratched areas were evaluated under light microscopy. The areas of these foci of wound closure in each culture conditions were quantified using MultiGauge v3.1 software (Fuji Photo Film Co., Ltd.) and compared to the corresponding areas in control cells.

2.8. Quantitative reverse transcriptional-polymerase chain reaction (RT-PCR)

Total RNA was extracted from NCI-H727 treated with RAD001 and/or U0126 for 12 h using TRIZOL reagent (Invitrogen, CA, USA) and a reverse transcriptional reaction was conducted using a QuantiTect reverse transcription kit (Qiagen, Hilden, Germany) and a PTC-200 Peltier Thermal Cycler DNA Engine (MJ Research Inc., Watertown, MA). Real-time PCR was carried out using the LightCycler System (Roche Diagnostics, Mannheim, Germany) and a QuantiTect SYBR Green PCR Master Mix (Qiagen). The primer sequences were summarized in Table 1. The ribosomal protein L13A (RPL13A) was used as an internal control and mRNA level of each condition was calculated as a ratio of *RPL13A* level compared with control levels.

2.9. Statistical analysis

The statistical analysis about the results of proliferation assay and wound healing assay was analyzed with Scheffe test (StatView 5.0J software, SAS Institute Inc., NC, USA) and Student *t* test (Microsoft Excel). Statistical significance was defined as $P < 0.05$.

3. Results

3.1. Expression of neuroendocrine markers in NET cell lines

We first confirmed the neuroendocrine features of two NET cell lines NCI-H727 and COLO320 used in our present study using immunocytochemistry. We examined three neuroendocrine markers chromogranin A, NSE and synaptophysin and all of these markers were detected in the cytoplasm of both cell lines (Fig. 1).

Table 1
Sequences of primers in this study.

Gene	GenBank No.	PCR primers
MMP2	NM_001127891	5′-ATAACCTGGATGCCGTCGTG-3′ 5′-AGCCTAGCCAGTCGGATTTG-3′
MMP9	NM_004994	5′-GACGTCTTCCAGTACCGA-3′ 5′-GGATGTCATAGGTCACGTAGC-3′
RPL13A	NM_012423	5′-CCTGGAGGAGAAGAGGAAAG-3′ 5′-TTGAGGACCTCTGTGTATTT-3′

3.2. Antitumor efficacy of RAD001 and MEK inhibitors in NET cell lines

We examined the anti-tumor effects and their concentration-dependency of RAD001 and U0126 in NCI-H727 and COLO320 (Fig. 2A and B, respectively). RAD001 significantly decreased the number of cells at 9th day of treatment in NCI-H727 and at 3rd day in COLO320 in the range of 1–100 nM, compared to the control levels (Fig. 2A). As for U0126, the cell growth was significantly inhibited at 3rd day with 1 μM in NCI-H727 and with 100 nM and 10 μM in COLO320 (Fig. 2B). Therefore, based upon these results, we determined the concentrations of these reagents as follows: RAD001, 100 nM; U0126, 1 μM (NCI-H727) or 10 μM (COLO320). The combined treatment of RAD001 with U0126 demonstrated a significant inhibition in both NCI-H727 and COLO320 for 3 days, compared to the other groups (Fig. 2C). Additionally, CI values in all conditions were smaller than 1.0 in both of the cell lines studied (Table 2).

3.3. Intracellular mechanisms of synergistic effects of mTOR and MEK inhibitors in NET cell lines

We demonstrated the synergic inhibition of cell proliferation by combined treatment of mTOR inhibitors with MEK inhibitors as described above. We then examined the status of the factors involved in Akt/mTOR and MEK/ERK signaling pathways at protein levels in order to clarify the alterations of signal transduction factors expression following the treatment. We first examined the time-dependency and determined the adequate time of simultaneous treatment in two of NET cell lines (NCI-H727, 6 h; COLO320, 3 h; data not shown). The status of mTOR-related factor expression was subsequently evaluated and the results were summarized as follows (Fig. 3): (a) RAD001 markedly inhibited the phosphorylation of mTOR and its downstream factors, S6 and 4EBP1, and U0126 also inhibited that of ERK. (b) RAD001 induced an activation of Akt and ERK. (c) U0126 similarly induced the expression of p-Akt and p-mTOR, especially in COLO320, but decreased that of p-S6 and p-4EBP1. (d) The combined treatment inhibited both RAD001-induced ERK activation and U0126-induced mTOR activation and demonstrated additive inhibition of the phosphorylation of both S6 and 4EBP1.

3.4. Effects of the treatment on cell cycle related protein expression

In order to investigate the effects of the combined treatment on cell cycle, we detected cell cycle related proteins when simultaneously treated. In NCI-H727 cells, RAD001 treatment induced the expression of Cyclin D1, which was inhibited or decreased by U0126 treatment such as phospho-ERK expression (Fig. 4). However, both reagents suppressed the expression of Cyclin D1 in COLO320. Regarding Cyclin B1, both RAD001 and U0126 treatment decreased its expression and their combination resulted in further reduction.

3.5. Effects of the treatment on cell migration activity

Results of wound healing assay demonstrated that cell migration activities were suppressed in single reagent treated cells (Fig. 5A) and the combined treatment resulted in significantly higher inhibition/suppression of cell migration than single treatment ($P < 0.05$: Fig. 5B).

3.6. Effects of the treatment on MMPs mRNA expression

We examined the effects of these reagents on MMP2 and MMP9 expressions at mRNA levels in NCI-H727 in order to investigate the mechanisms of the inhibition of cell migration as demonstrated

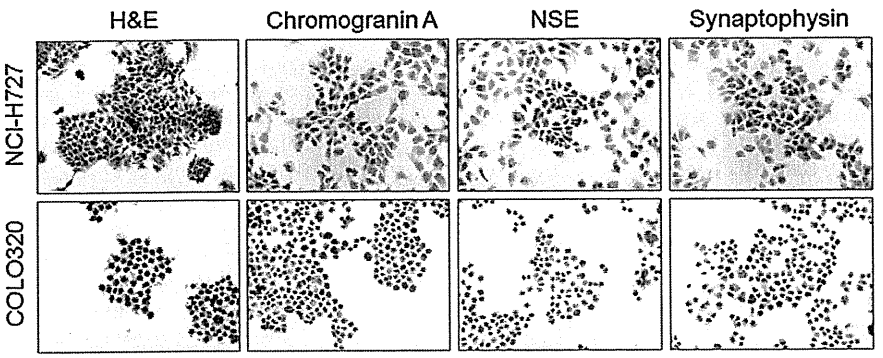

Fig. 1. Representative illustration of hematoxylin and eosin (H&E) staining and immunocytochemistry of neuroendocrine markers in NET cell lines. Both NCI-H727 and COLO320 cultured in 4-well plate were immunostained with three neuroendocrine markers, chromogranin A, NSE and synaptophysin. Original magnification, 100×.

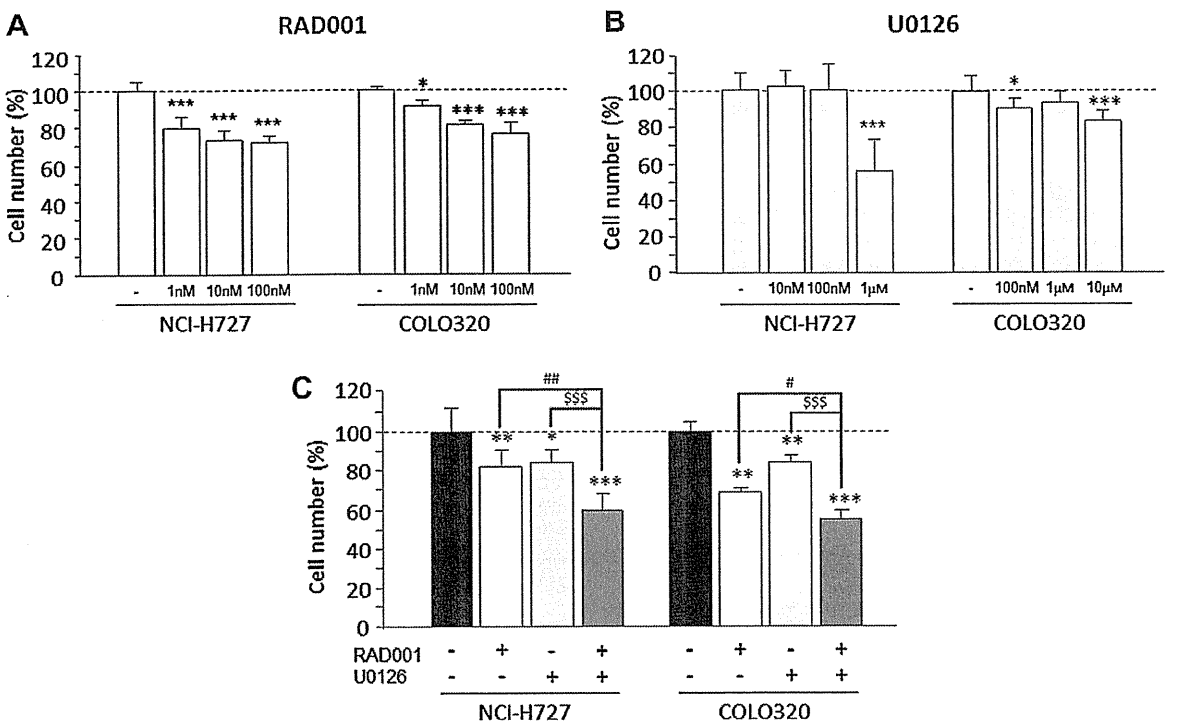

Fig. 2. Anti-tumor effects of RAD001 and U0126 treatment in NET cells. (A) RAD001 treatment (1–100 nM) in NCI-H727 at 9th day and in COLO320 at 3rd day. (B) U0126 treatment at the range of 10 nM to 1 μM in NCI-H727 and 100 nM to 10 μM in COLO320. (C) Combination treatment of RAD001 (100 nM) with U0126 [1 μM (NCI-H727) or 10 μM (COLO320)] at 3rd day. All data are shown as mean ($n = 6$). Error bars indicate SD. Statistical significances were calculated by Scheffe test. $^{*}P < 0.05$, $^{**}P < 0.01$ and $^{***}P < 0.001$, compared with control group; $^{\#}P < 0.05$ and $^{\#\#}P < 0.01$, compared with RAD001 treatment group; $^{\$\$\$}P < 0.001$, compared with U0126 treatment group.

above. Results were summarized in Fig. 6. RAD001 exerted no significant effects upon *MMP2* mRNA expression, whereas U0126 and the combination treatment significantly decreased that of MMP2. As for MMP9, both RAD001 and U0126 significantly decreased its expression and their simultaneous administration decreased it in an additive manner.

4. Discussion

We previously reported the subclassification of non-functioning NET cases using hierarchical clustering analysis based upon immunoreactivity of various factors involved in the regulation of cell proliferation (Iida et al., 2010). Briefly, non-functioning NETs were sub-classified into sstr-related group and mTOR activation-related group and the latter group may be considered to benefit from mTOR inhibitors. It is, however, also true that several investigators reported the potential limitation of the efficacy of mTOR inhibitors in NET cases (Duran et al., 2006). In our present study, we focused

Table 2
Combination index values of the combined effects of RAD001 with U0126 in NET cells.

Cell line	RAD001	U0126	Fractional affected	CI value
NCI-H727	1 nM	10 nM	0.266	0.003
	10 nM	100 nM	0.301	0.021
	100 nM	1 μM	0.402	0.144
COLO320	1 nM	100 nM	0.205	0.098
	10 nM	1 μM	0.289	0.089
	100 nM	10 μM	0.453	0.453

Note: CI < 1.0 indicates synergism, CI = 1.0 indicates additivity and CI > 1.0 indicates antagonism.

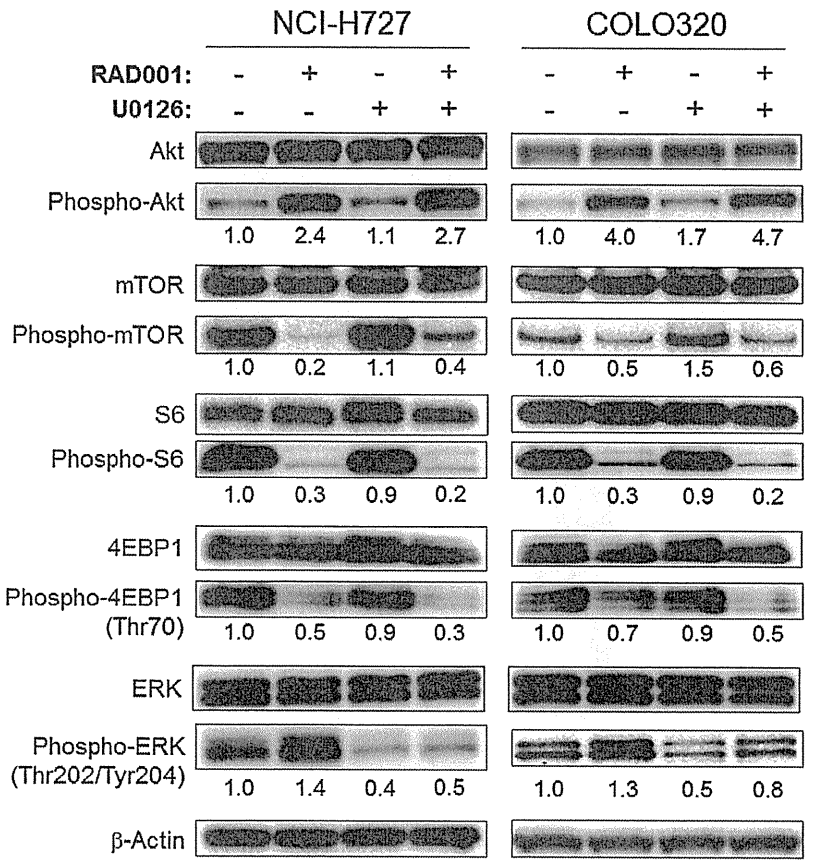

Fig. 3. Summary of the expression of phosphorylated factors in Akt/mTOR and MEK/ERK pathway when RAD001 and/or U0126 were treated. Phosphorylated forms of Akt, mTOR, S6, 4EBP1 and ERK were detected when RAD001 (100 nM) and U0126 [1 μM (NCI-H727) or 10 μM (COLO320)] were treated in NCI-H727 for 6 h and COLO320 for 3 h. The number under each band calculated using MultiGauge v3.1 software (Fuji Photo Film Co., Ltd.) indicated the intensity when the control bands were 1.0.

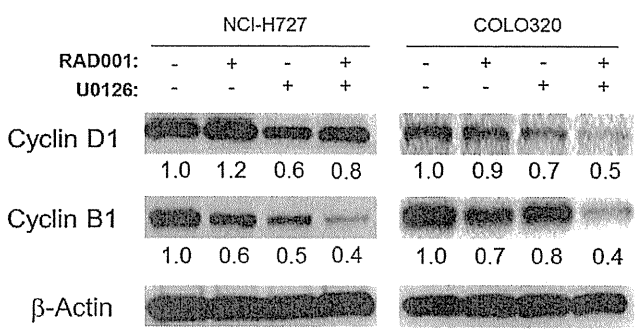

Fig. 4. Summary of the expression of cell cycle-related factors when RAD001 and/or U0126 were administered. The expressions of Cyclin D1 and Cyclin B1 as G1/S and G2/M phase markers, respectively, were detected when treated with RAD001 (100 nM) and U0126 [1 μM (NCI-H727) or 10 μM (COLO320)] for 24 h. The number under each band calculated using MultiGauge v3.1 software (Fuji Photo Film Co., Ltd.) indicated the intensity when the control bands were 1.0.

on one of the potential mechanisms of development of resistance to mTOR inhibitors, that is, a positive feedback loop from MEK/ERK pathway (Carracedo et al., 2008; Mi et al., 2009; O'Reilly et al., 2006; Wang et al., 2008) because the combined therapeutic effects of mTOR and MEK inhibitors has not been necessarily studied in NET.

The mechanism of therapeutic resistance to an inhibitor of Raf, an upstream factor of MEK, was recently reported in melanoma cells (Johannessen et al., 2010; Nazarian et al., 2010). These reports also indicated an involvement of the acquired resistance through activating a RTK (PDGFRβ was found in this study)-dependent survival pathway and reactivating MAPK pathway via Ras upregulation. In addition, U0126 has been known to cause an activation of PI3K/Akt/mTOR pathway in non-small cell lung carcinoma cells, as was previously reported by Meng et al. (2009). They also demonstrated the association of high levels of Akt activity with resistances to MEK inhibition. In our present study, single treatment of mTOR or MEK inhibitor resulted in a significant suppression of cell proliferation and their combination did demonstrate therapeutic effects in a synergistic manner because its CI values were smaller than 1.0. We first demonstrated that RAD001 inhibited an activation of mTOR but did activate Akt and ERK at the protein levels in both cell lines. As for MEK inhibition, U0126 suppressed ERK activation but did activate Akt and mTOR. These results indicated that between these two pathways, one induced the other pathway and the combined treatment inhibited the each pathway induced by the each reagent as expected. In addition, U0126 inhibited the activation of both S6 and 4EBP1, downstream factors of mTOR, as RAD001 did. Both of these factors have been known to be regulated by MEK/ERK pathway, as previously reported (Herbert et al., 2002; Wang et al., 2001). Zitzmann et al. previously demonstrated the combination treatment of RAD001 with a Raf inhibitor Raf265 in NET cells (Zitzmann et al., 2010). In our present study, RAD001 increased the activation of Akt but not that of ERK at the concentration of 100 nM for 2 and 24 h in NCI-H727, respectively. We examined the antitumor effects of RAD001 in a time-dependent manner and detected ERK activation by the treatment of this reagent for 3, 6 and 12 h (data not shown). In addition, ERK activation

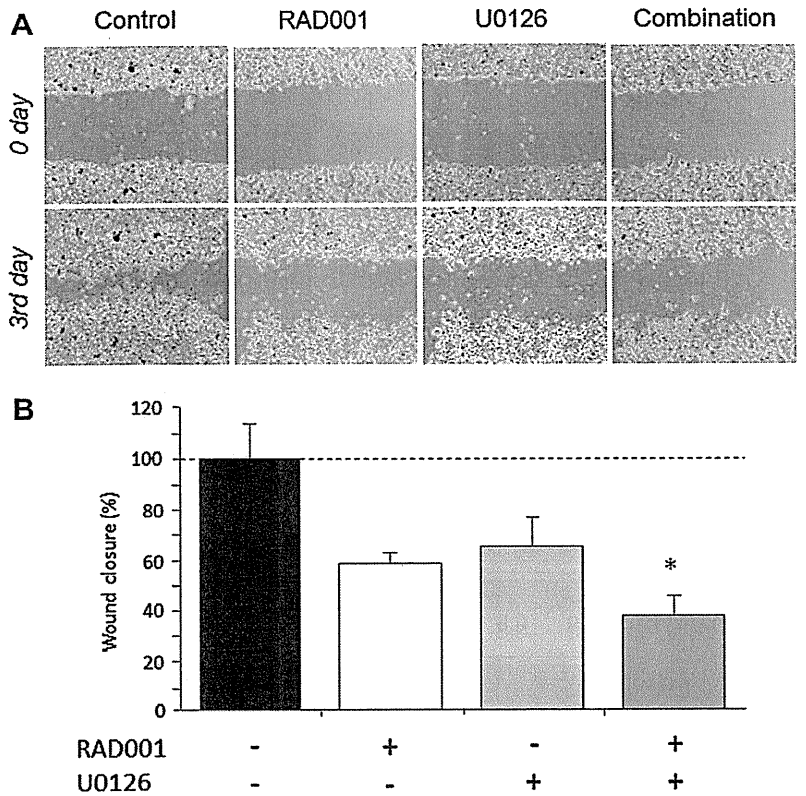

Fig. 5. Summary of the results of migration assay in NCI-H727. (*A*) Representative illustrations of migration assay in NCI-H727 at the 3rd day and (*B*) the results of statistical analysis ($P < 0.05$, Scheffe test; $n = 3$).

was detected when RAD001 and mTOR/PI3K inhibitor NVP-BEZ235 were treated in other types of NET cell lines (i.e. BON1 and GOT1). Zitzmann et al. also demonstrated that Raf265 induced Akt activation, suggesting that, as described in our present study, an inhibition of Ras–Raf–MEK–ERK pathway may result in a positive feedback loop for PI3K–Akt–mTOR pathway. These results all indicated that the combined inhibition of both pathways could be effective in NET cells.

It is widely known that both mTOR and MEK inhibitors induce cell cycle arrest (Hoshino et al., 2001; Yu et al., 2001). Therefore, in this study, we explored alterations of the factors involved in the process of cell cycle arrest. Cell cycle was arrested by an administration of a single inhibitor and furthermore, the combined treatment additively suppressed the expression of G1/S and G2/M phase positive regulators, Cyclin D1 and Cyclin B1, respectively. These results all indicated that the anti-tumor activity of this dual inhibition of mTOR and MEK pathway was caused by the cell cycle arrest. We further demonstrated the differences of their effects on Cyclin D1 expression between in two types of NET cells. In NCI-H727 cell line, U0126 decreased the expression of Cyclin D1, whereas RAD001 induced its amount to the similar level of phospho-ERK. These findings suggested that Cyclin D1 expression was predominantly regulated by MEK/ERK pathway in NCI-H727, as previously reported by Lavoie et al. (1996).

Some patients with well-differentiated non-functioning NETs may clinically present with metastatic disease at initial visits and therapeutic options in these cases are markedly limited (Reidy et al., 2009). No standard therapy is currently available, which makes it important to explore the possibility of the combined treatment studied in our present *in vitro* study of NET cells. In glioma cells, the combination of a Raf inhibitor and RAD001 significantly suppressed the invasive properties of tumor cells (Hjelmeland et al., 2007). In our present study, the combination of RAD001 and U0126 significantly decreased NET cell migration in addition to synergistic inhibition of cell proliferation, which may also suggest an additional benefit of the combination of mTOR and MEK inhibitors for the treatment of NET patients. In our present study, we focused on MMPs expression involved in the inhibitory mechanisms of cell migration. In Lewis lung carcinoma cells, *MMP2* mRNA expression was not influenced by mTOR inhibitor rapamycin and MEK inhibitor decreased its expression as we demonstrated in NCI-H727 (Zhang et al., 2004). As for MMP9, its expression was reported to be significantly correlated with PI3K–Akt–mTOR pathway in hepatocellular carcinoma cells (Chen et al., 2009). In addition, the decrement of *MMP9* mRNA expression by U0126 and inhibitors of PI3K, wortmannin and LY294002, was also previously reported in ovarian and breast cancer cells (Thant et al., 2000; Reddy et al., 1999). Therefore, as we demonstrated, the inhibition of cell migration by RAD001 and U0126 was associated with the decrement of MMP2 and 9.

Yao and co-researchers recently reported that RAD001 administration was clinically effective for progression-free survival and the ratio of severe adverse events in progressive advanced pancreatic NETs in phase III clinical trials (Yao et al., 2011). However it is also true that mTOR inhibitors were associated with limitations caused by Akt and ERK activation in NET cells as reported in our present study. All of these findings including those of our present study suggest that the expression of activated Akt and ERK could be evaluated in surgical pathology specimens of NET cases prior to RAD001 treatment and the combined agent may be selected based upon the results of these evaluations. When Akt activation is detected in tumor cells using immunohistochemistry in biopsy specimens, somatostatin analogue may be administered because they were reported to inactivate Akt and to further stabilize symptoms (Arnold et al., 2000; Charland et al., 2001). The combined treatment of RAD001 with octreotide LAR (Novartis) has been evaluated in phase III clinical trial and its results demonstrated a

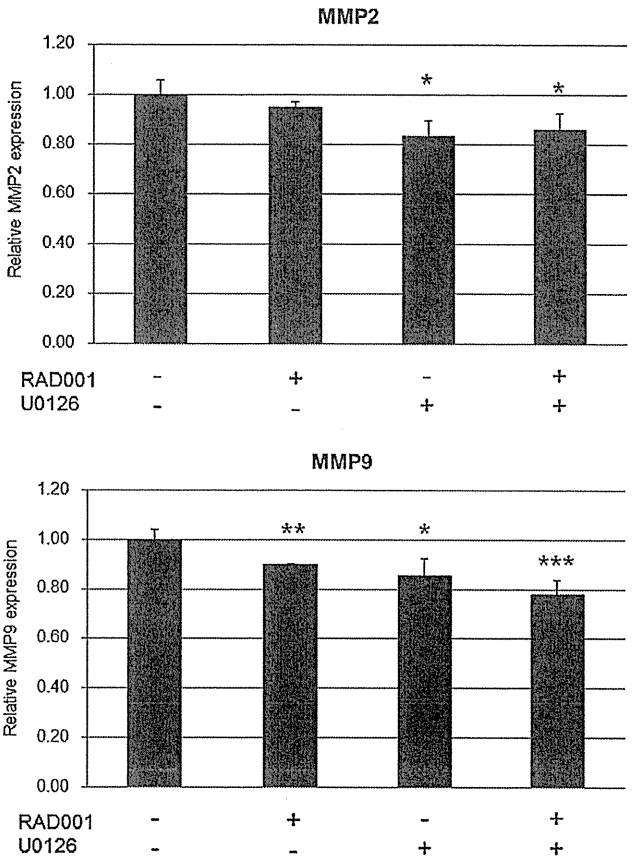

Fig. 6. Summary of mRNA levels of MMP2 and 9 in NCI-H727 when RAD001 and/or U0126 were treated. 100 nM of RAD001 and 1 μM of U0126 were respectively or simultaneously administered for 12 h and the expression levels of *MMP2* and *9* mRNA were evaluated. These experiments were performed in triplicate. $^{*}P < 0.05$, $^{**}P < 0.01$ and $^{***}P < 0.001$, compared with control group (Student *t* test).

significant clinical improvement in advanced NET patients (Pavel et al., 2011). Regarding Ras–Raf–MEK–ERK pathway, a MEK or a Raf inhibitor may be combined with an mTOR inhibitor (Hjelmeland et al., 2007). It is true that MEK or Raf inhibitors have not yet been clinically applied in any tumors but the development of the combined therapy has been expected. In addition, the effects detected in our present study may be also detected in other types of malignancies and the correlation of the findings obtained with neuroendocrine features of the tumors cells, that is, the synthesis and secretion of peptide hormones needs to be clarified by further investigations.

In summary, we firstly demonstrated the synergistic suppression of cell proliferation and invasive properties in the dual inhibition of mTOR and MEK in NET cell lines by suppressing the compensatory induction or activation of the pathway caused by suppression of mTOR or MEK signaling pathways. In our previous study, mTOR or ERK activation was detected in 63.5% and 34.6% of NET cases, respectively (Iida et al., 2010), and combined treatment may be effective when applied to the patients with NET.

Acknowledgements

We appreciate Novartis Oncology for supplying RAD001 for our analysis. We appreciate Miki Mori and Erina Iwabuchi (Department of Pathology, Tohoku University School of Medicine) for their skillful technical assistances despite the unprecedented enormous damages inflicted upon Tohoku University, Sendai, Japan by March 11th earthquake, which interrupted this study.

References

Amato, R.J., Jac, J., Giessinger, S., Saxena, S., Willis, J.P., 2009. A phase 2 study with a daily regimen of the oral mTOR inhibitor RAD001 (everolimus) in patients with metastatic clear cell renal cell cancer. Cancer 115, 2438–2446.

Arnold, R., Simon, B., Wied, M., 2000. Treatment of neuroendocrine GEP tumours with somatostatin analogues. Digestion 62, 84–91.

Bjornsti, M.A., Houghton, P.J., 2004. The TOR pathway: a target for cancer therapy. Nat. Rev. Cancer 4, 335–348.

Carracedo, A., Ma, L., Teruya-Feldstein, J., Rojo, F., Salmena, L., Alimonti, A., Egia, A., Sasaki, A.T., Thomas, G., Kozma, S.C., Papa, A., Nardella, C., Cantley, L.C., Baselga, J., Pandolfi, P.P., 2008. Inhibition of mTORC1 leads to MAPK pathway activation through a PI3K-dependent feedback loop in human cancer. J. Clin. Invest. 118, 3065–3074.

Chan, H.Y., Grossman, A.B., Bukowski, R.M., 2010. Everolimus in the treatment of renal cell carcinoma and neuroendocrine tumors. Adv. Ther. 27, 495–511.

Chang, Q., Chapman, M.S., Miner, J.N., Hedley, D.W., 2010. Antitumour activity of a potent MEK inhibitor RDEA110/BAY 869766 combined with rapamycin in human orthotopic primary pancreatic cancer xenograft. BMC Cancer 10, 515–526.

Charland, S., Boucher, M.J., Houde, M., Rivard, N., 2001. Somatostatin inhibits Akt phosphorylation and cell cycle entry, but not p42/p44 mitogen-activated protein (MAP) kinase activation in normal and tumoral pancreatic acinar cells. Endocrinology 142, 121–128.

Chen, J.S., Wang, Q., Fu, X.H., Huang, X.H., Chen, X.L., Cao, L.Q., Chen, L.Z., Tan, H.X., Li, W., Bi, J., Zhang, L.J., 2009. Involvement of PI3K/PTEN/AKT/mTOR pathway in invasion and metastasis in hepatocellular carcinoma: association with MMP-9. Hepatol. Res. 39, 177–186.

Chou, T.C., 2006. Theoretical basis, experimental design, and computerized simulation of synergism and antagonism in drug combination studies. Pharmacol. Rev. 58, 621–681.

Chou, T.C., 2010. Drug combination studies and their synergy quantification using the Chou–Talalay method. Cancer Res. 70, 440–446.

Chou, T.C., Talalay, P., 1984. Quantitative analysis of dose-effect relationships: the combined effects of multiple drugs or enzyme inhibitors. Adv. Enzyme Regul. 22, 27–55.

Ciuffreda, L., Di Sanza, C., Incani, U.C., Milella, M., 2010. The mTOR pathway: a new target in cancer therapy. Curr. Cancer Drug Targets 10, 484–495.

Duran, I., Kortmansky, J., Singh, D., Hirte, H., Kocha, W., Goss, G., Le, L., Oza, A., Nicklee, T., Ho, J., Birle, D., Pond, G.R., Arboine, D., Dancey, J., Aviel-Ronen, S., Tsao, M.S., Hedley, D., Siu, L.L., 2006. A phase II clinical and pharmacodynamic study of temsirolimus in advanced neuroendocrine carcinomas. Br. J. Cancer 95, 1148–1154.

Grozinsky-Glasberg, S., Franchi, G., Teng, M., Leontiou, C.A., Ribeiro de Oliveira, A., Dalino Jr., P., Salahuddin, N., Korbonits, M., Grossman, A.B., 2008. Octreotide and the mTOR inhibitor RAD001 (everolimus) block proliferation and interact with the Akt-mTOR-p70S6K pathway in a neuro-endocrine tumour cell line. Neuroendocrinology 87, 168–181.

Hartley, D., Cooper, G.M., 2002. Role of mTOR in the degradation of IRS-1: regulation of PP2A activity. J. Cell Biochem. 85, 304–314.

Herbert, T.P., Tee, A.R., Proud, C.G., 2002. The extracellular signal-regulated kinase pathway regulates the phosphorylation of 4E-BP1 at multiple sites. J. Biol. Chem. 277, 11591–11596.

Hess, G., Herbrecht, R., Romaguera, J., Verhoef, G., Crump, M., Gisselbrecht, C., Laurell, A., Offner, F., Strahs, A., Berkenblit, A., Hanushevsky, O., Clancy, J., Hewes, B., Moore, L., Coiffier, B., 2009. Phase III study to evaluate temsirolimus compared with investigator's choice therapy for the treatment of relapsed or refractory mantle cell lymphoma. J. Clin. Oncol. 27, 3822–3829.

Hjelmeland, A.B., Lattimore, K.P., Fee, B.E., Shi, Q., Wickman, S., Keir, S.T., Hjelmeland, M.D., Batt, D., Bigner, D.D., Friedman, H.S., Rich, J.N., 2007. The combination of novel low molecular weight inhibitors of RAF (LBT613) and target of rapamycin (RAD001) decreases glioma proliferation and invasion. Mol. Cancer Ther. 6, 2449–2457.

Hoshino, R., Tanimura, S., Watanabe, K., Kataoka, T., Kohno, M., 2001. Blockade of the extracellular signal-regulated kinase pathway induces marked G1 cell cycle arrest and apoptosis in tumor cells in which the pathway is constitutively activated upregulation of p27Kip1. J. Biol. Chem. 276, 2686–2692.

Iida, S., Miki, Y., Ono, K., Akahira, J., Suzuki, T., Ishida, K., Watanabe, M., Sasano, H., 2010. Novel classification based on immunohistochemistry combined with hierarchical clustering analysis in non-functioning neuroendocrine tumor patients. Cancer Sci. 101, 2278–2285.

Jayaraman, T., Marks, A.R., 1993. Rapamycin-FKBP12 blocks proliferation, induces differentiation, and inhibits cdc2 kinase activity in a myogenic cell line. J. Biol. Chem. 268, 25385–25388.

Jin, N., Jiang, T., Rosen, D.M., Nelkin, B.D., Ball, D.W., 2009. Dual inhibition of mitogen-activated protein kinase kinase and mammalian target of rapamycin in differentiated and anaplastic thyroid cancer. J. Clin. Endocrinol. Metab. 94, 4107–4112.

Johannessen, C.M., Boehm, J.S., Kim, S.Y., Thomas, S.R., Wardwell, L., Johnson, L.A., Emery, C.M., Stransky, N., Cogdill, A.P., Barretina, J., Caponigro, G., Hieronymus, H., Murray, R.R., Salehi-Ashtiani, K., Hill, D.E., Vidal, M., Zhao, J.J., Yang, X., Alkan, O., Kim, S., Harris, J.L., Wilson, C.J., Myer, V.E., Finan, P.M., Root, D.E., Roberts, T.M., Golub, T., Flaherty, K.T., Dummer, R., Weber, B.L., Sellers, W.R., Schlegel, R., Wargo, J.A., Hahn, W.C., Garraway, L.A., 2010. COT drives resistance to RAF inhibition through MAP kinase pathway reactivation. Nature 468, 968–973.

Kikade, C.W., Castillo-Martin, M., Puzio-Kuter, A., Yan, J., Foster, T.H., Gao, H., Sun, Y., Ouyang, X., Gerald, W.L., Cordon-Cardo, C., Abate-Shen, C., 2008. Targeting AKT/mTOR and ERK/MAPK signaling inhibits hormone-refractory prostate cancer in a preclinical mouse model. J. Clin. Invest. 118, 3051–3064.

Lasithiotakis, K.G., Sinnberg, T.W., Schittek, B., Flaherty, K.T., Kulms, D., Maczey, E., Garbe, C., Meier, F.E., 2008. Combined inhibition of MAPK and mTOR signaling inhibits growth, induces cell death, and abrogates invasive growth of melanoma cells. J. Invest. Dermatol. 128, 2013–2023.

Lavoie, J.N., L'Allemain, G.L., Brunet, A., Müller, R., Pouysségur, J., 1996. Cyclin D1 expression is regulated positively by the p42/44MAPK and negatively by the p38/HOGMAPK pathway. J. Biol. Chem. 271, 20608–20616.

Liang, C.C., Park, A.Y., Guan, J.L., 2007. *In vitro* scratch assay: a convenient and inexpensive method for analysis of cell migration *in vitro*. Nat. Protoc. 2, 329–333.

Loewith, R., Jacinto, E., Wullschleger, S., Lorberg, A., Crespo, J.L., Bonenfant, D., Oppliger, W., Jenoe, P., Hall, M.N., 2002. Two TOR complexes, only one of which is rapamycin sensitive, have distinct roles in cell growth control. Mol. Cell 10, 457–468.

Meng, J., Peng, H., Dai, B., Guo, W., Wang, L., Ji, L., Minna, J.D., Chresta, C.M., Smith, P.D., Fang, B., Roth, J.A., 2009. High level of AKT activity is associated with resistance to MEK inhibitor AZD6244 (ARRY-142886). Cancer Biol. Ther. 21, 2073–2080.

Mi, R., Ma, J., Zhang, D., Li, L., Zhang, H., 2009. Efficacy of combined inhibition of mTOR and ERK/MAPK pathways in treating a tuberous sclerosis complex cell model. J. Genet. Genomics 36, 355–361.

Moreno, A., Akcakanat, A., Munsell, M.F., Soni, A., Yao, J.C., Meric-Bernstam, F., 2008. Antitumor activity of rapamycin and octreotide as single agents or in combination in neuroendocrine tumors. Endocr. Relat. Cancer 15, 257–266.

Nazarian, R., Shi, H., Wang, Q., Kong, X., Koya, R.C., Lee, H., Chen, Z., Lee, M.K., Attar, N., Sazegar, H., Chondon, T., Nelson, S.F., McArthur, G., Sosman, J.A., Ribas, A., Lo, R.S., 2010. Melanomas acquire resistance to B-RAF(V600E) inhibition by RTK or N-RAS upregulation. Nature 468, 973–979.

O'Reilly, K.E., Rojo, F., She, Q.B., Solit, D., Mills, G.B., Smith, D., Lane, H., Hofmann, F., Hicklin, D.J., Ludwig, D.L., Baselga, J., Rosen, N., 2006. MTOR inhibition induces upstream receptor tyrosine kinase signaling and activates Akt. Cancer Res. 66, 1500–1508.

Pavel, M., Peeters, M., Hörsch, D., Van Cutsem, E., Öberg, K., Jehl, V., Klimovsky, J., Yao, J., 2011. Everilumus + Octreotide LAR vs placebo + Octreotide LAR in patients with advanced neuroendocrine tumors (NET): Updated results of a randomized double-blind, placebo-controlled, multicenter phase III trial (RADIANT-2). The 8th Annual ENETS Conferences, C86.

Pouysségur, J., Dayan, F., Mazure, N., 2006. Hypoxia signaling in cancer and approaches to enforce tumour regression. Nature 441, 437–443.

Quinn, L.A., Moore, G.E., Morgan, R.T., Woods, L.K., 1979. Cell lines from human colon carcinoma with unusual cell products, double minutes, and homogeneously staining regions. Cancer Res. 39, 4914–4924.

Reddy, K.B., Krueger, J.S., Kondapaka, S.B., Diglio, C.A., 1999. Mitogen-activated protein kinase (MAPK) regulates the expression of progelatinase B (MMP-9) in breast epithelial cells. Int. J. Cancer 82, 268–273.

Reidy, D.L., Tang, L.H., Saltz, L.B., 2009. Treatment of advanced disease in patients with well-differentiated neuroendocrine tumors. Nat. Clin. Pract. 6, 143–152.

Sunayama, J., Matsuda, K., Sato, A., Tachibana, K., Suzuki, K., Narita, Y., Shibui, S., Sakurada, K., Kayama, T., Tomiyama, A., Kitanaka, C., 2010. Crosstalk between the PI3K/mTOR and MEK/ERK pathways involved in the maintenance of self-renewal and tumorigenecity of glioblastoma stem-like cells. Stem Cells 28, 1930–1939.

Thant, A.A., Nawa, A., Kikkawa, F., Ichigotani, Y., Zhang, Y., Sein, T.T., Amin, A.R., Hamaguchi, M., 2000. Fibronectin activates matrix metalloproteinase-9 secretion via the MEK1-MAPK and the PI3K-Akt pathways in ovarian cancer cells. Clin. Exp. Metastasis 18, 423–428.

Theodoropoulou, M., Zhang, J., Laupheimer, S., Paez-Pereda, M., Erneux, C., Florio, T., Pagotto, U., Stalla, G.K., 2006. Octreotide, a somatostatin analogue, mediates its antiproliferative action in pituitary tumor cells by altering phosphatidylinositol 3-kinase signaling and inducing Zac1 expression. Cancer Res. 66, 1576–1582.

Thomson, A.W., Turnauist, H.R., Raimondi, G., 2009. Immunoregulatory functions of mTOR inhibition. Nat. Rev. Immunol. 9, 324–337.

Vilella-Bach, M., Nuzzi, P., Fang, Y., Chen, J., 1999. The FKBP12-rapamycin-binding domain is required for FKBP12-rapamycin-associated protein kinase activity and G_1 progression. J. Biol. Chem. 274, 4266–4272.

von Wichert, G., Jehle, P.M., Hoeflich, A., Koschnick, S., Dralle, H., Wolf, E., Wiedenmann, B., Boehm, B.O., Adler, G., Seufferlein, T., 2000. Insulin-like growth factor-I is an autocrine regulator of chromogranin A secretion and growth in human neuroendocrine tumor cell. Cancer Res. 60, 4573–4581.

Wang, L., Gout, I., Proud, C.G., 2001. Cross-talk between the ERK and p70 S6 kinase (S6K) signaling pathways. J. Biol. Chem. 276, 32670–32677.

Wang, X., Hawk, N., Yue, P., Kauh, J., Ramalingam, S.S., Fu, H., Khuri, F.R., Sun, S.Y., 2008. Overcoming mTOR inhibition-induced paradoxical activation of survival signaling pathways enhances mTOR inhibitors' anticancer efficacy. Cancer Biol. Ther. 7, 1952–1958.

Wullschleger, S., Loewith, R., Hall, M.N., 2006. TOR signaling in growth and metabolism. Cell 124, 471–484.

Yao, J.C., Phan, A.T., Chang, D.Z., Wolff, R.A., Hess, K., Gupta, S., Jacobs, C., Mares, J.E., Landgraf, A.N., Rashid, A., Meric-Bernstam, F., 2008. Efficacy of RAD001 (everolimus) and octreotide LAR in advanced low- to intermediate-grade neuroendocrine tumors: results of a phase II study. J. Clin. Oncol. 26, 4311–4318.

Yao, J.C., Shah, M.H., Ito, T., Bohas, C.L., Wolim, E.M., Van Cutsem, E., Hobday, T.J., Okusaka, T., Capdevila, J., de Vries, E.G., Tomassetti, P., Pavel, M.E., Hoosen, S., Haas, T., Lincy, J., Lebwohl, D., Öberg, K., 2011. RAD001 in Advanced Neuroendocrine tumors, third trial (RADIANT-3) study group. Everolimus for advanced pancreatic neuroendocrine tumors. N. Engl. J. Med. 10, 514–523.

Yu, K., Toral-Barza, L., Discafani, C., Zhang, W.G., Skotnicki, J., Frost, P., Gibbons, J.J., 2001. MTOR, a novel target in breast cancer: the effect of CCI-779, an mTOR inhibitor, in preclinical models of breast cancer. Endocr. Relat. Cancer 8, 249–258.

Zhang, D., Bar-Eli, M., Meloche, S., Brodt, P., 2004. Dual regulation of MMP-2 expression by the type 1 insulin-like growth factor receptor: the phosphatidylinositol 3-kinase/Akt and Raf/ERK pathways transmit opposing signals. J. Biol. Chem. 279, 19683–19690.

Zhang, H., Bajraszewski, N., Wu, E., Wang, H., Mosenman, A.P., Dabora, S.L., Griffin, J.D., Kwiatkowski, D.J., 2007. PDGFRs are critical for PI3K/Akt activation and negatively regulated by mTOR. J. Clin. Invest. 117, 730–738.

Zitzmann, K., von Rüden, J., Brand, S., Göke, B., Lichtl, J., Spöttl, G., Auernhammer, C.J., 2010. Compensatory activation of Akt in response to mTOR and Raf inhibitors – a rationale for dual-targeted therapy approaches in neuroendocrine tumor disease. Cancer Lett. 295, 100–109.

Zutzmann, K., De Toni, E.N., Brand, S., Göke, B., Meinecke, J., Spöttl, G., Meter, H.H., Auernhammer, C.J., 2007. The novel mTOR inhibitor RAD001 (Everolimus) induces antiproliferative effects in human pancreatic neuroendocrine tumor cells. Neuroendocrinology 85, 54–60.

JJCO Japanese Journal of Clinical Oncology

Jpn J Clin Oncol 2012;42(3)168–174
doi:10.1093/jjco/hyr197
Advance Access Publication 4 January 2012

Breast Ultrasonographic and Histopathological Characteristics Without Any Mammographic Abnormalities

Kentaro Tamaki[1,2,3,*], Takanori Ishida[2], Minoru Miyashita[2], Masakazu Amari[2], Noriaki Ohuchi[2], Yoshihiko Kamada[1], Kano Uehara[1], Nobumitsu Tamaki[1] and Hironobu Sasano[3]

[1]Department of Breast Surgery, Nahanishi Clinic, Okinawa, [2]Department of Surgical Oncology, Tohoku University Graduate School of Medicine and [3]Department of Pathology, Tohoku University Hospital, Miyagi, Japan

*For reprints and all correspondence: Kentaro Tamaki, 1-1 Seiryo-machi, Aoba-ku, Sendai, Miyagi 980-8574, Japan. E-mail: nahanisikenta@yahoo.co.jp

Received October 13, 2011; accepted December 13, 2011

Objective: We evaluated ultrasonographic findings and the corresponding histopathological characteristics of breast cancer patients with Breast Imaging Reporting and Data System (BI-RADS) category 1 mammogram.
Methods: We retrospectively reviewed the ultrasonographic findings and the corresponding histopathological features of 45 breast cancer patients with BI-RADS category 1 mammogram and 537 controls with mammographic abnormalities. We evaluated the ultrasonographic findings including mass shape, periphery, internal and posterior echo pattern, interruption of mammary borders and the distribution of low-echoic lesions, and the corresponding histopathological characteristics including histological classification, hormone receptor and human epidermal growth factor receptor 2 status of invasive ductal carcinoma and ductal carcinoma *in situ*, histological grade, mitotic counts and lymphovascular invasion in individual cases of BI-RADS category 1 mammograms and compared with those of the control group.
Results: The ultrasonographic characteristics of the BI-RADS category 1 group were characterized by a higher ratio of round shape ($P < 0.001$), non-spiculated periphery ($P = 0.021$), non-interruption of mammary borders ($P < 0.001$) and non-attenuation ($P = 0.011$) compared with the control group. A total of 52.6% of low-echoic lesions were associated with spotted distribution in the BI-RADS 1 group, whereas 25.8% of low-echoic lesions were associated with spotted distribution in the control group ($P = 0.012$). As for histopathological characteristics, there was a statistically higher ratio of triple-negative subtype ($P = 0.021$), and this particular tendency was detected in histological grade 3 in the BI-RADS category 1 group ($P = 0.094$).
Conclusion: We evaluated ultrasonographic findings and the corresponding histopathological characteristics for BI-RADS category 1 mammograms and noted significant differences among these findings in this study. Evaluation of these ultrasonographic and histopathological characteristics may provide a more accurate ultrasonographic screening system for breast cancer in Japanese women.

Key words: breast US – BI-RADS category 1 mammogram – histopathological characteristics

INTRODUCTION

The incidence of breast cancer has increased worldwide, which is partly considered to be due to mass screening programs resulting in the discovery of clinically occult or early breast lesions (1). Early clinical detection of breast cancer through screening has therefore led to the detection of the tumor at a relatively earlier clinical stage. The effectiveness of screening mammography on reduction in mortality by breast cancer has been well established in both Western countries and Japan (2). Mammography has thus become the gold standard for